YIELDING AND FLOW OF THE B.C.C. METALS AT LOW TEMPERATURES

Hans Conrad
Materials Sciences Laboratory
Aerospace Corporation
El Segundo, California

ABSTRACT

The available experimental data on the mechanical behavior of the B.C.C. transition metals at low temperatures ($< 0.25\ T_m$) are reviewed and analyzed to establish the rate-controlling mechanism responsible for the strong temperature and strain rate dependence of the yield and flow stresses. The activation energy H, activation volume v^*, and frequency factor ν were determined as a function of the thermal component of the stress τ^*. It was found that H_o ($\tau^* = 1$ Kg/mm^2) $\simeq 0.1\ \mu b^3$ where μ is the shear modulus and b the Burgers vector, $v^* \simeq 50\ b^3$ at $\tau^* = 2$ Kg/mm^2, increasing rapidly to values in excess of $100\ b^3$ at lower stresses and decreasing to 2-5 b^3 at high stresses (50-60 Kg/mm^2) and $\nu = 10^6 - 10^{12}$ sec^{-1}, the higher values of ν generally being associated with the purer materials. H and v^* as a function of stress were independent of structure. This along with other observations indicates that thermally-activated overcoming of the Peierls-Nabarro stress is the rate-controlling mechanism. The values of H_o and the change in H with stress at low stresses are in agreement with those predicted by Seeger's model for the nucleation of kinks. The Peierls-Nabarro stress and kink energy derived from the experimental data are approximately $10^{-2}\mu$ and $4 \times 10^{-2}\ \mu b^3$ respectively.

The experimental data suggest that the yield point in the B.C.C. metals is associated with the sudden multiplication of dislocations by the double cross-slip mechanism, which in turn is controlled by the motion of dislocations through the lattice. Stress-strain curves for mild steel calculated on the basis of this mechanism are in good agreement with the experimental curves.

YIELDING AND FLOW OF THE B.C.C. METALS AT LOW TEMPERATURES

Hans Conrad
Materials Sciences Laboratory
Aerospace Corporation
El Segundo, California

Introduction

A distinguishing feature of the B.C.C. metals, as compared to the close-packed (C.P.H. and F.C.C.) metals, is the strong effect of temperature and strain rate on the yield stress at low temperatures ($T < 0.2\ T_m$); see, for example, Figs. 1 and 2. (T is the test temperature and T_m is the melting temperature.) An understanding of this difference is of technological, as well as scientific interest, for the ductile-to-brittle transition in the B.C.C. metals is related to the strong temperature and strain rate dependence of the yield stress.

A number of thermally-activated dislocation mechanisms have been proposed to account for the strong temperature and strain rate dependence of the yield stress of the B.C.C. metals. In chronological order, these are:

1. Breaking away from an interstitial atmosphere (1-4)
2. Overcoming the Peierls-Nabarro stress (5-9)†
3. Non-conservative motion of jogs (11-13)
4. Overcoming interstitial precipitates (14)
5. Cross-slip (15)

There is some experimental support for each of these mechanisms, making it difficult to decide which one is actually rate-controlling. From a review

†Heslop and Petch (10) first suggested that the strong temperature dependence of the yield and flow stress in iron might be due to a high Peierls-Nabarro stress. However, they attributed the temperature dependence to a change in width of the dislocation with temperature rather than the contribution of thermal fluctuations to overcoming of the Peierls-Nabarro stress. Their suggestion does not account for the strong effect of strain rate on the yield stress.

of the experimental data available at the time for iron, Conrad (6) concluded that best overall agreement was for thermally-activated overcoming of the Peierls-Nabarro stress. Subsequent work on iron (8,16) supported this conclusion. More recently, Conrad and Hayes (9) analyzed the available data for the Group VA (V, Nb, Ta) and Group VIA (Cr, Mo, W) metals and again concluded that the rate-controlling mechanism at low temperatures was overcoming the Peierls-Nabarro stress. A similar conclusion was reached by Basinski and Christian (5) for iron and Christian and Masters (7) for the Group VA metals.

In the present paper pertinent data for all the B.C.C. transition metals are reviewed (including some more recent data [7,13,17-19])† and the question of the rate-controlling mechanism during low temperature deformation re-examined.

Experimental Data

I. Effect of Temperature on Yield and Flow Stresses

1. Micro-deformation

Employing a strain sensitivity of 4×10^{-6} and a strain rate of $\sim 10^{-3}$ sec^{-1}, Brown and Ekvall (15) found that the stress-strain behavior of ultrapure ($\sim$ 0.004 wt % interstitials) and impure ($\sim$ 0.04 wt % interstitials) iron consisted of three distinct regions; Fig. 3.

A. σ_E†† is the stress where a hysteresis loop is first observed upon loading and unloading and represents the first evidence of dislocation motion. σ_E was only observed after previous straining ($\epsilon = 10^{-4}$ to 5×10^{-2}).

---

†Sources of data in addition to those mentioned in the text are given at the end of the bibliography. Also given there are the references pertaining to the Figures.

††Throughout the present paper σ will be used to designate tensile stress and τ shear stress. It will be assumed that $\tau = \frac{1}{2}\sigma$. Similarily, $\dot{\epsilon}$ is the tensile strain rate and $\dot{\gamma}$ the shear strain rate; $\dot{\gamma} = 0.7\ \dot{\epsilon}$.

B. σ_A is the stress at which a permanent strain first occurs; i.e. the lowest stress at which the hysterisis loop does not close. This is generally the same as the stress at which a deviation from linearity can be measured and is usually called the proportional limit.

C. σ_F is the commonly called yield or flow stress.

Brown and Ekvall found that σ_E was independent of temperature (between 300° and 78°K) for both the impure and pure irons. The variation of σ_A with temperature is shown in Fig. 4. σ_A for the locked state (undeformed impure iron) here exhibits about the same temperature dependence as that previously reported (20,21) for the lower yield stress (of annealed or strain-aged states) and the subsequent flow stress of various impure irons (C + N > 0.015 wt %) and steels.† On the other hand, σ_A for the unlocked (deformed) state has a lower temperature dependence than that for yielding or for subsequent flow. Additional evidence that the proportional limit σ_A after prestraining has a weaker temperature dependence than the flow stress σ_F of iron has been reported by Conrad and Frederick (8), Fig. 5, and Kitajima (22).

2. Macro-deformation

The yield or flow stress τ of B.C.C. metals can be considered to consist of three components (6,10,20,21):

$$\tau = \tau^* (T,\dot{\gamma}) + \tau_\mu + Kd^{-\frac{1}{2}} \qquad (1)$$

τ^* is the thermal component which depends on temperature T and strain rate $\dot{\gamma}$ and is associated with thermally-assisted overcoming of short-range obstacles. τ_μ represents the athermal component associated with long-range stress fields, is independent of strain rate, and varies with temperature only through the temper-

†Data on the other B.C.C. metals also indicate that the proportional limit of annealed impure (> 0.02 wt % interstitials) material has a temperature dependence similar to that for the subsequent yield and flow stresses (9,20).

ature variation of the shear modulus μ. $Kd^{-\frac{1}{2}}$ is the component representing the grain size effect. K is the slope of the plot of the yield or flow stress versus the reciprocal of the square root of the grain size d and for annealed impure material is relatively independent of temperature and strain rate, when compared to τ^* (21, 23-26). When K is independent of grain size, $Kd^{-\frac{1}{2}}$ gives the Hall-Petch relation (27, 28). There are, however, indications (29) that K for both the lower yield stress and flow stress is a function of the grain size and, therefore, that the effect of grain size is not given by the simple Hall-Petch equation.

In the present discussion we are principally concerned with the effect of temperature on the thermal component τ^* and wish to separate it from the others. This is accomplished by subtracting the stress at a given temperature T from that at some reference temperature T^o (6,20) (assuming that K is relatively independent of temperature), i.e.

$$\tau_T - \tau_{T^o} = \tau^* (T,\dot{\gamma}) - \tau^* (T^o,\dot{\gamma}) = \Delta\tau^* (T,\dot{\gamma}) \qquad (2)$$

Typical results on iron and tungsten are shown in Figs. 5 and 6. Similar plots have been developed previously for iron (20) and the Group VA and VIA metals (9, 20). τ^* as a function of temperature is then derived from such plots by taking $\tau^* = 0$ at the temperature T_o, obtained by extrapolating plots of $\log \left(\frac{\partial\tau^*}{\partial T}\right)$ versus T to a value of $\sim 5 \times 10^{-3}$ Kg/(mm^2 - ^oK), where $\frac{1}{\tau}\frac{d\tau}{dT} \approx \frac{1}{\mu}\frac{d\mu}{dT}$ and hence $\tau \approx \tau_\mu$. ($\frac{\partial\tau^*}{\partial T}$ is obtained by graphical differentiation of average curves similar to those in Figs. 5 and 6.) Plots of τ^* for yielding versus temperature for a strain rate of $\sim 10^{-4}$ sec^{-1} derived in this manner from the available experimental data are given in Figs. 7 and 8. It is here seen that for the Group VA metals the variation of τ^* with temperature is relatively independent of purity and grain size (i.e. whether the specimen is single or polycrystalline), while for the Group VIA metals and iron, τ^* as a function of temperature is clearly dependent on purity and grain

size. For the Group VIA metals and iron, the upper limit of τ^* at a given temperature is for polycrystals with interstitial contents ≥ 0.02 wt %; the lower limit is for single and polycrystals with less than 0.005 wt % interstitials. Single crystals and polycrystals with intermediate impurity levels exhibited a variation of τ^* with temperature between these two limits. In general, for the impure materials τ^* at a given temperature was less for single crystals than for polycrystals of the same impurity content. Figs. 5 and 10 show that previous thermal treatment and deformation may also influence the temperature dependence of τ^*.

Values of T_o (to the nearest 50°K) for a strain rate of 10^{-4} sec^{-1} are given in Table I. For the Group VIA metals and iron, T_o for the pure materials is less than that for the impure materials, whereas for the Group V metals there is no significant effect of impurity content T_o. This difference and the difference in the effect of impurity content on the temperature dependence of τ^* may be related to the higher solubility of interstitials in the Group VA metals compared to the Group VIA metals and iron.

From Table I it is seen that the ratio T_o/T_m is 0.22 ± 0.04 for all impure polycrystalline B.C.C. metals. In a previous paper (9) it was shown that the yield stresses of all the impure polycrystalline B.C.C. metals correlate rather well on a single curve when τ^* is plotted versus the parameter $(T-T_o)/T_m$.

Values of τ_o^* obtained by extrapolating the curves of Figs. 7-9 to 0°K are given in Table II. Because of the rapid increase in τ^* at very low temperatures, there is some uncertainty associated with these values. However, if one plots the logarithm of τ^* versus temperature, an approximately linear region occurs at low temperatures (see Fig. 11) allowing for an easier extrapolation. Extrapolation of this linear region to 0°K gives values of τ_o^* slightly higher than those based on the linear plots; see Table II. Both methods yield values of τ_o^*

of the order of $10^{-2}\mu$.

II. Effect of Strain Rate on the Yield and Flow Stresses

Fig. 2 shows typical variation of the strain rate parameter $\Delta\sigma/\Delta \ln \dot{\epsilon}$, ($\Delta\sigma$ is the incremental increase in yield or flow stress for an increase in strain rate from $\dot{\epsilon}_1$ to $\dot{\epsilon}_2$) with temperature for the B.C.C. metals.† It initially increases with decrease in temperature below T_o, goes through a maximum, and then decreases again, approaching zero as the temperature goes to absolute zero. It depends on structure (i.e. on impurities and on thermal and mechanical history) in a similar manner as does the parameter $\frac{\Delta\tau^*}{\Delta T}$; compare, for example, the effect of strain on $\Delta\sigma/\Delta \ln \dot{\epsilon}$ and on $\frac{\Delta\tau^*}{\Delta T}$ for iron in Figs. 2 and 5.

Another type of experiment which also gives the relationship between the yield stress and strain rate is the so-called delay-time test employed by Wood and Clark (31) and others (32). In general, the parameter $\Delta\sigma/\Delta \ln t_d$ obtained from such tests, where t_d is the delay time for yielding, has a similar value and exhibits the same trends as does the parameter $\Delta\sigma/\Delta \ln \dot{\epsilon}$.

III. Activation Energy, Activation Volume and Frequency Factor for Deformation

1. General

It is now generally accepted that the deformation of metals may be thermally activated, and if a single mechanism is rate-controlling, one can write for the shear strain rate $\dot{\gamma}$

$$\dot{\gamma} = \rho b \dot{s} = \rho b s \nu^* \exp\left(-\frac{H(\tau,T)}{kT}\right) \qquad (3)$$

where ρ is the density of dislocations contributing to the deformation, b the Burgers vector, $\dot{s}$ the average velocity of the dislocations, s the product of the number of places where thermal activation can occur per unit length of dislocation

†More detailed data on the variation of $\frac{\Delta\sigma}{\Delta \ln \dot{\epsilon}}$ with temperature are found in Refs. 5,7,8, and 13.

and the area swept out per successful thermal fluctuation, ν^* the frequency of vibration of the dislocation segment involved in the thermal activation, and H the activation enthalpy (energy) which may be a function of the shear stress τ and the temperature T. For the B.C.C. metals it has been established (6,8,9,16) that H is primarily a function of the effective shear stress τ^*, (i.e. the thermal component of the yield or flow stress) given by the difference between the applied stress τ and the long range internal stress τ_μ; i.e. $\tau^* = \tau - \tau_\mu$. Further, one can show that (33)

$$H = - k \left(\frac{\partial \ln \dot{\gamma}/\nu}{\partial 1/T} \right)_{\tau^*} \tag{4}$$

$$= - kT^2 \left(\frac{\partial \ln \dot{\gamma}/\nu}{\partial \tau} \right)_T \left(\frac{\partial \tau^*}{\partial T} \right)_{\dot{\gamma}} \tag{4a}$$

Rearranging Eq. 3 and differentiating, one obtains

$$- \frac{dH}{d\tau^*} = k\, T \left(\frac{\partial \ln \dot{\gamma}/\nu}{\partial \tau} \right)_T \tag{5}$$

$$= \frac{k \ln (\dot{\gamma}/\nu)}{\left(\frac{\partial \tau^*}{\partial T} \right)_{\dot{\gamma}}} \tag{5a}$$

where $\nu = \rho b s \nu^*$ and $- \frac{dH}{d\tau^*}$ is defined as the activation volume v^*. The value of ν can be obtained from the relations

$$H = kT \ln(\nu/\dot{\gamma}) \tag{6}$$

or

$$- T \left(\frac{\partial \ln \dot{\gamma}}{\partial \tau} \right)_T \left(\frac{\partial \tau^*}{\partial T} \right) = \ln (\nu/\dot{\gamma}) \tag{6a}$$

i.e from the slope of a plot of H versus T or a plot of $\left(\frac{\partial \tau^*}{\partial T} \right)_{\dot{\gamma}}$ versus $\frac{1}{T} \left(\frac{\partial \tau}{\partial \ln \dot{\gamma}} \right)_T$. If ν is relatively independent of temperature and stress per se, the values of H, v^* and ν can then be derived from the relationships between stress, temperature and strain rate obtained from the usual mechanical tests.† For polycrystalline

†The values of H, v^* and the product $s\nu^*$ can also be obtained from measurements of the effect of stress and temperature on dislocation velocity by replacing the strain rate $\dot{\epsilon}$ in Eqs. 4-6 with the velocity $\dot{s}$.

B.C.C. metals (and also single crystals) a reasonable assumption is that $\tau = \frac{1}{2}\sigma$, and $\gamma = 0.7\,\epsilon$, where σ is the tensile stress and ϵ is the tensile strain; also $\left(\frac{\partial \tau^*}{\partial T}\right)_{\dot{\gamma}}$ is approximated by $\left(\frac{\partial \tau}{\partial T}\right)_{\dot{\gamma}}$, for $\frac{d\tau_\mu}{\partial T}$ is small compared to $\left(\frac{\partial \tau^*}{\partial T}\right)$.

2. Activation Energy, H

The variation of H with τ^* obtained from the available experimental data is shown in Figs. 12-18. Essentially identical results were obtained from the use of either Eq. 4 or 4a, supporting the validity of the assumptions inherent in these equations. The curves drawn in these figures represent the author's interpretation of the variation of H with τ^* indicated by the data points. There is, however, some doubt as to whether a change in curvature actually occurs at the low stress and, for the most part, the data suggest equally well a rather rapid increase in H as τ^* approaches zero. Of particular significance in Figs. 12-18 is that, within the scatter of the data, H as a function of τ^* is independent of the yielding or flow phenomena considered (microcreep, delay time, proportional limit, upper yield stress, flow and dislocation velocity) and of the structure (impurity content, grain size, and previous thermal or mechanical history) for a given metal. In Fig. 19 it is seen that H_o, the value of H at $\tau^* = 1$ Kg/mm^2, is approximately equal to $0.1\,\mu b^3$, when comparing the various B.C.C. metals.[†]

A number of investigators (2,6,34-36) have reported that the activation energy for yielding in iron decreases in a linear manner with the logarithm of the total applied stress τ. For comparison, plots of H versus log τ^* are given in Fig. 20 for the various impure polycrystalline B.C.C. metals.[††] It is here seen that for such plots there appears to be two linear regions, one at very low stresses

[†]The shear modulus values were derived from the relation $\mu = \frac{3}{8}E$, where E is the Young's modulus at T_o taken from Ref. 30.

[††]The values of H and τ^* plotted in Fig. 20 were taken from the average curves drawn in Figs. 12-18.

and the other at high stresses, with a transition region in the vicinity of $\tau^* = 1\text{-}5$ Kg/mm^2. The slope in the high stress region is about 10 times that in the low stress region. Extrapolation of the straight lines at high stresses to H = 0 gives values of τ_o^* in reasonable agreement with those obtained by the other two methods; see Table II.

3. Activation volume, v*

Typical variation of v* with τ^* is shown for Ta, W, and Fe in Figs. 21-23. There was agreement between values obtained from Eq. 5 and Eq. 5a. and from graphical differentiation of the curves of Figs. 12-18, except at the lowest values of τ^*.† Fig. 24 shows that the activation volume as a function of stress is similar for all the B.C.C. metals. The values given here were taken from average curves such as those drawn in Figs. 21-23. It is seen from Fig. 24 that, for all of the B.C.C. metals, v* is about 50 b^3 at $\tau^* = 2$ Kg/mm^2, increasing rapidly to values in excess of 100 b^3 at lower values of stress and decreasing with stress to values as low as 2-5 b^3. Again, as for H, v* as a function of stress is independent of the yielding or flow phenomena considered and of the structure (i.e. of mechanical and thermal history).

4. Frequency Factor, ν

Typical proportionality between H and temperature obtained for the B.C.C. metals is shown in Fig. 25. Plots of the average curves of H vs T for all the impure polycrystalline B.C.C. metals are given in Fig. 26. Average values of ν derived from such plots for both pure (< 0.005 wt %) and impure (> 0.02 wt %) materials are given in Table III.

Additional evidence of the proportionality between H and temperature is provided by the variation of the ductile-to-brittle transition temperature in

---

†This disagreement will be discussed in a subsequent section.

the B.C.C. metals with strain rate. Generally, a straight line is obtained when the logarithm of the strain rate is plotted versus the reciprocal of the transition temperature (37,38), suggesting a rate equation of the form $\dot{\epsilon} = Ae^{-H/kT}$. Taking the logarithm of both sides of this equation and rearranging, one obtains $H = kT \ln A/\dot{\epsilon}$ (see Fig. 27), which agrees with Eq. 6 when $A = \nu$. This is consistent with the analysis of Eqs. 3-6, if the transition from ductile to brittle behavior occurs at a constant stress. The values of ν derived from the effect of strain rate on the ductile-to-brittle transition are given in Table IV. They are in reasonable agreement with those obtained from the yield and flow stress measurements listed in Table III, indicating that the ductile-to-brittle transition temperature is determined by the dynamic motion of dislocations, as has been proposed by Cottrell (40) and Petch (24).

Discussion

1. Rate-Controlling Mechanism

The fact that the various relationships of Eqs. 3-6 gave the same values of H, v^* and ν indicates that the postulated assumptions are valid, at least to a first approximation. Specifically, this supports the contention that during the low temperature deformation ($< 2.0\ T_m$) of the B.C.C. transition metals a single dislocation mechanism is rate-controlling and that ν is relatively independent of stress and temperature per se. Furthermore, the fact that identical values of H and v^* were obtained for all yielding and flow phenomena (and the ductile-to-brittle transition) indicates that the same dislocation mechanism is controlling in all cases and that this is associated with the motion of dislocations through the lattice, as distinct from a generation mechanism, such as breaking away from an interstitial atmosphere. Finally, the fact that H and v^* as a function of stress were independent of structure (i.e. thermal and mechanical history) strongly

suggests that the rate-controlling mechanism is overcoming the inherent resistance of the lattice, i.e. overcoming the Peierls-Nabarro stress. Further support for the Peierls-Nabarro mechanism is that dislocations in the B.C.C. metals are often observed to lie along the close-packed directions (41-43). A summary of the experimental evidence negating the other mechanisms mentioned in the Introduction is given in Table V.

A possible thermally-activated mechanism for overcoming the Peierls-Nabarro stress (energy) is that originally proposed by Seeger (44) to explain the Bordoni peak in F.C.C. metals and is shown in Fig. 28. It involves the formation of a pair of kinks in a dislocation line lying in a close-packed direction by the combined action of thermal fluctuations and the applied stress, and the subsequent lateral propagation of the kinks along the dislocation line, resulting in the forward motion of the dislocation. Seeger (44) calculated the activation energy for this process at low stresses to be

$$H = H_K \left[1 + \tfrac{1}{4} \log \left(\frac{16\, \tau_\rho^o}{\pi \tau^*}\right)\right]^{\dagger} \qquad (7)$$

where H_K is the energy of a single kink and τ_ρ^o is the Peierls-Nabarro stress at 0^oK. Furthermore, Seeger gives

$$H_K = \frac{2a}{\pi} \left(\frac{2E_o\, ab\, \tau_\rho^o}{\pi}\right)^{\frac{1}{2}} \qquad (8)$$

---

†The thermal component of the stress τ^* has been substituted for the total stress τ in Seeger's equation.

and $$H_{PN} = \frac{\tau_p^o \, ab^2}{2\pi} \qquad (9)$$

$$= \frac{H_K^2 \, \pi^2 \, b}{16a^2 E_o} \qquad (9a)$$

where $2H_{PN}$ is the Peierls-Nabarro energy per atomic length, a the distance between close-packed rows, b the Burgers vector and E_o the line energy of a dislocation. Taking the average value of τ_o^* (from Table II) for τ_p^o and taking $E_o = \frac{1}{2}\mu b^2$, one obtains from Eqs. 7 and 8, H_o ($\tau^* = 1$ Kg/mm^2) $\simeq 0.1\ \mu b^3$, in good agreement with measured values of H_o; see Table VI. Furthermore, from Eqs. 7 and 8 one obtains $H_K = 3\text{-}4 \times 10^{-2}\ \mu b^3$ and from Eq. 9, $H_{PN} = 1\text{-}2 \times 10^{-3}\ \mu b^3$; again see Table VI. Taking the derivative of Eq. 7 with respect to τ^* gives

$$-\frac{dH}{d\tau^*} = v^* = \frac{1}{4}\frac{H_K}{\tau^*} \, . \qquad (10)$$

Values of H_K derived from the values of v^* at $\tau^* = 1$ Kg/mm^2 are also given in Table VI and are in agreement with those obtained from Eqs. 7 and 8. For comparison, values of H_K derived from the slope of the plots of H vs log τ^* (Fig. 20) at low stresses (< 1 Kg/mm^2) are approximately 1/6 to 1/3 those calculated using Eqs. 7 and 8, while those derived from the slope at high stresses (> 10 Kg/mm^2) are about 3 to 4 times larger. Agreement occurs in the intermediate stress range ($\tau^* = 1\text{-}5$ Kg/mm^2), where the plots show curvature.

The good agreement between the values of H_o and H_K obtained from the various relationships (Eqs. 7-10) indicates rather strongly that the nucleation of kinks is the rate-controlling mechanism during low temperature deformation of the B.C.C. metals. Although the derived values of τ_p^o, H_K and H_{PN} are somewhat higher than those usually given for close-packed metals (45), they are in accord with those calculated using the original Peierls-Nabarro equations (46) and the

more recent calculations of Kuhlmann-Wilsdorf (47) and Hobart and Celli (48). The good agreement between the values of H_o and H_K obtained using only experimental data and those obtained using $E_o = \frac{1}{2}\mu b^2$ indicates that the line energy in the B.C.C. metals is very nearly $\frac{1}{2}\mu b^2$.

According to Seeger (44) the width w of a kink is given by

$$w = \tfrac{1}{2}\, a \left(\frac{E_o\, b}{H_{PN}}\right)^{\frac{1}{2}} \tag{11}$$

and the critical separation ℓ^* of the kinks during thermal activation is

$$\ell^* = \frac{w}{\pi} \log\left(\frac{32\, H_{PN}}{\tau^*\, b^3}\right) \tag{12}$$

$$= \frac{H - H_K}{2\, H_{PN}} \tag{12a}$$

The values of w and of ℓ^*(at $\tau = 1$ Kg/mm^2) obtained from Eqs. 11, 12 and 12a using the average values of H_K, H_{PN} and H ($\tau^* = 1$ Kg/mm^2) from Table VI and taking $E_o = \frac{1}{2}\mu b^2$ are given in Table VII. It is here seen that w = 7-10 b and $\ell^*(\tau^* = 1$ Kg/mm^2) = 12-22 b, which are quite reasonable. Again of significance is the good agreement between values of ℓ^* from Eqs. 12 and 12a.

For the Peierls-Nabarro mechanism the frequency factor can be given by

$$\nu = \rho b \left[\left(\frac{1}{\ell^*}\right)\left(Lb\right)\left(\frac{b}{\ell^*}\, v_d\right)\right] \tag{13}$$

where ρ is the density of dislocations participating in the deformation, b the Burgers vector, ℓ^* the length of dislocation segment involved in the thermal activation, L the maximum lateral spread of the kinks and ν_d the Debye frequency. The first term within the brackets represents the number of places per unit dislocation length where thermal fluctuations may nucleate a loop of length ℓ^*; the second term is the area of the slip plane swept-out per successful thermal fluctuation; the third term is the frequency of vibration of a segment of length ℓ^*. Taking $\rho = 10^9$ cm^{-2}, $\ell^* = 10b$, $L = 10^{-4}$ cm and $\nu_d = 10^{13}$ sec^{-1}, one obtains $\nu = 10^8$ sec^{-1}, in agreement with that observed experimentally for many materials; see Tables III and IV.

Since H and v^* as a function of τ^* were independent of structure, the effect of impurities, precipitates, grain size, dislocations and other aspects of previous thermal or mechanical history on the temperature dependence of the yield or flow stress is then due to a change in the frequency factor ν, i.e. in the number of dislocations ρ participating in the deformation or in the lateral distance L a kink can move before encountering an obstacle. In this regard, Conrad and Frederick (8) investigated the effect of straining and of interstitial precipitates in iron on the temperature dependence of τ^*. Some of their results are given in Fig. 3, which shows that a weaker temperature dependence results from straining and from the presence of precipitates. Figs. 29 and 30 (taken from their paper) show that the weaker temperature dependence is associated with a larger value of ν, given by the slope of the plot of H vs temperature. From the relation $\nu = \rho b s v^*$ and taking the value of sv^* derived from the dislocation velocity measurements of Stein and Low (50), they obtained values of ρ, and their increase with strain (see Table VIII) in agreement with dislocation densities determined by Keh and Weissman (42) by thin-film electron microscopy, indicating

that the increase in ν was due primarily to an increase in ρ. They further concluded from their results that precipitates represented good sources for dislocations, in agreement with observations of Leslie (51) and Van Torne and Thomas (52).

From Table III it is seen that the weaker temperature dependence of τ^* for single crystals or pure polycrystals as compared to impure polycrystals in the Group VIA metals and iron is associated with a frequency factor that is larger by 3 to 5 orders of magnitude. These larger values of ν cannot be due entirely to a greater dislocation density ρ, for this would require unreasonably large values for ρ. Rather, it appears that this difference in ν is primarily due to larger values of L for the pure as compared to the impure materials, suggesting that interstitial atoms or precipitates influence the extent to which the kinks can spread before encountering an obstacle. Besides acting as obstacles to kink motion, the interstitial atoms or precipitates may induce cross-slip, which in turn limits the dislocation loop length on the slip plane. Of interest in this regard are the observations of Schadler and Low (19), who report that under some conditions dislocations in tungsten crystals can move long distances without multiplying, in agreement with the high values of ν given in Table III for single crystals of tungsten.

All of the above supports overcoming the Peierls-Nabarro stress by thermally-activated nucleation of kinks as the rate-controlling mechanism in the B.C.C. metals at low temperatures. However, explanation is needed for the fact that in the vicinity of T_o (i.e. $\tau^* = 0$) H, for the most part, does not increase as rapidly with decrease in stress (or increase in temperature) as is expected from the values of v^* or the straight line portion of the H versus temperature curves at lower temperatures. As indicated earlier, the scatter in the data allow for a more rapid increase in H than is indicated by the curves

drawn in Figs. 12-18. The low values of H for stresses only slightly greater than zero may then simply reflect the difficulty in defining $\tau^* = 0$ exactly. Also, ν may actually decrease with increase in temperature (or decrease in stress).† On the other hand, a different mechanism may become rate-controlling in the very low stress range. Additional work is needed to resolve this problem.

Finally, one needs to explain the much smaller temperature dependence of the proportional limit after straining and the fact that σ_E, as defined by Brown and Ekvall (15), is independent of temperature. Also, in recent investigations on the determination of H as a function of stress in Ta by creep tests, Chambers (39) found a spectrum of activation energies for very small strain rates (10^{-6} - 10^{-11} sec^{-1}) rather than a single activation energy.†† There are two possible explanations for these various effects:

(1) These phenomena represent the motion of those specific dislocations located in the most favorable internal stress fields and the applied stress primarily gives direction to the motion of these dislocations and does not contribute significantly to the thermally-activated process.

(2) Another easier mechanism is rate-controlling at the very low stress levels, for example the lateral motion of kinks, as proposed by Brailsford (53), or the lateral motion of jogs as suggested by Chambers (54).

In both cases the easier motion would soon die out and, to obtain gross macroscopic flow, the more difficult mechanism of nucleating kinks would become rate-controlling. The rapid strain hardening associated with the early part of the stress-strain curve

---

†The change in ν may be the result of straining at different temperatures (or stresses) rather than the effect of stress or temperature per se.

††As an upper limit, Chambers (39) reported an H versus stress relationship in agreement with that given in Fig. 14.

would then be an exhaustion hardening rather than an interaction hardening, which occurs subsequently during macro-flow. Here, also, additional research is needed to resolve this question.

2. Yield Point and Work Hardening

The fact that K in Eq. 1 is relatively independent of temperature and that the activation energy and activation volume as a function of stress are the same for all deformation phenomena suggest that the yield point in the B.C.C. metals is not due to the thermally-assisted unpinning of dislocations from their interstitial atmosphere, as proposed by Cottrell (1), but rather results from the sudden multiplication of dislocations by the double cross-slip mechanism of Koehler (55) and Orowan (56), as proposed by Johnston and Gilman (57) for LiF. In this latter model the multiplication of dislocations is controlled by their motion through the lattice, in agreement with the experimental facts. As pointed out previously (16) three factors favor the occurrence of such a yield point in the B.C.C. metals:

(1) Initially there exists only a small number of dislocations which can contribute to the plastic flow, due to the "pegging" of the available dislocations by interstitial precipitates (as distinct from pinning by an interstitial atmosphere).

(2) The dislocation density contributing to the plastic flow increases very rapidly with strain. This is inherent in the double cross-slip mechanism for multiplication, and has been observed experimentally in iron by Keh and Weissman (42) and in molybdenum by Benson (58).

(3) The change in stress for a given change in dislocation velocity $\left[\left(\frac{\partial \sigma}{\partial \ln \dot{\varepsilon}}\right)\right.$ or $\left.\left(\frac{\partial \sigma}{\partial \ln \dot{\varepsilon}}\right)\right]$ is relatively large; see Fig. 2.

To check the proposed interpretation of the yield point, stress-strain curves for mild steel were calculated (16) using Eqs. 1 and 3 and the available

information on the activation energy as a function of stress (Fig. 18), the value of sv^* derived from etch pit measurements in silicon-iron (6), the increase in dislocation density with strain (42) and the increase in flow stress associated with the increase in dislocation density (42). The good agreement between the calculated and experimental curves is shown in Fig. 31. Since only plastic strain was considered, the upper yield point was taken as the stress at a plastic strain of 10^{-4}, which is approximately the observed pre-yield micro-strain in iron and steel.

Acknowledgement

The author wishes to express appreciation to B. L. Mordike, G. A. Sargent, P. J. Sherwood, A. A. Johnson, R. Chambers, J. W. Christian and B. C. Masters for submitting data previous to publication. He also wishes to acknowledge the valuable assistance of G. Stone in making calculations and plotting graphs.

TABLE I

T_o and the ratio T_o/T_m for pure (< 0.005 wt % interstitials) and impure (> 0.02 wt % interstitials) B.C.C. metals for a strain rate of 10^{-4} sec^{-1}.

Metal	T_m, °K	T_o, °K		T_o/T_m	
		Pure	Impure	Pure	Impure
V	2137	---	500	----	0.23
Nb	2741	500	500	0.18	0.18
Ta	3269	600	600	0.18	0.18
Cr	2148	---	500	----	0.26
Mo	2883	450	700	0.16	0.24
W	3683	500	850	0.14	0.23
Fe	1810	300	350	0.16	0.19

TABLE II

Extrapolated values of τ^* to 0°K, τ_o^*, obtained by different methods.

Metal	$\mu^\dagger$	τ_o^*, Kg/mm^2				τ_o^*(Avg.)/μ
	x 10^3 Kg/mm^2	τ^* vs T	log τ^* vs T	H vs log τ^*	Avg.	x 10^{-2}
V	5.2	60	65	60	62	1.19
Nb	4.0	58	65	60	61	1.52
Ta	7.0	60	67	80	69	.99
Cr	11.4	79	90	80	83	.73
Mo	12.7	78	105	85	89	.70
W	15.7	100	165	100	122	.78
Fe	7.4	49	65	60	58	.78

†The value of the shear modulus was taken as $\mu = 3/8$ E, where E is Youngs modulus at 300°K taken from data by Tietz and Wilson (30).

TABLE III

The frequency factor ν for the B.C.C. metals obtained from yield or flow stress measurements.

Metal	Authors	ν (sec^{-1}) Pure Single or Polycrystals	ν (sec^{-1}) Impure Polycrystals
V	Present	---	10^{6}
	Christian and Masters (7)	---	10^{10}
Nb	Present	10^{6}	10^{6}
	Christian and Masters (7)	---	10^{8}
Ta	Present	10^{8}	10^{8}
	Chambers (39)	10^{7}	---
	Christian and Masters (7)	---	10^{11}
	Mordike (13)	10^{9}	---
Cr	Present	---	10^{9}
Mo	Present	10^{11}	10^{6}
W	Present	10^{11}	10^{7}
Fe	Present	10^{11}	10^{8}
	Basinski and Christian (5)	---	10^{8}
	Conrad (6)	---	$10^{8} - 10^{9}$
	Lean, Plateau and Crussard (38)	---	$10^{8} - 10^{10}$

TABLE IV

Values of ν derived from the effect of strain rate on the ductile-to-brittle transition temperature (Data from Refs. 37 and 38.)

Metal	ν (sec^{-1})
Cr	10^{10}
Mo	$10^{8} - 10^{12}$
W	10^{12}
Fe	$10^{8} - 10^{12}$

TABLE V

Summary of evidence against specific mechanisms which have been proposed as rate-controlling during the low temperature deformation of the B.C.C. metals.

Mechanism	Contrary Evidence
Breaking-away from an interstitial atmosphere	1. All yielding and flow phenomena exhibit the same values of H and v*. 2. H and v* are independent of interstitial content. 3. H and v* are the same for the mobility of dislocations as determined by etch pits as for initial yielding.
Non-conservative motion of jogs	1. H and v* are independent of structure. 2. H and v* for yielding and flow are the same as for the mobility of edge dislocations, which do not move non-conservatively.
Overcoming interstitial precipitates	1. H and v* are independent of impurity content. 2. H and v* are independent of the quantity of interstitial precipitates. 3. τ^* decreases with increase in quantity of precipitates.
Cross-slip	1. H and v* for yielding and flow are the same as for the mobility of edge dislocations, which cannot cross-slip.

TABLE VI

Values of H_o, H_K and H_{PN} derived from the experimental data.

Metal	b Å	μb^3† ergs x 10^{-12}	$H_o(\tau^* = 1\ Kg/mm^2)/\mu b^3$ Eqs. 7 & 8 x 10^{-2}	$H_o(\tau^* = 1\ Kg/mm^2)/\mu b^3$ Figs. 12-18 x 10^{-2}	$H_K/\mu b^3$ Eq. 7 x 10^{-2}	$H_K/\mu b^3$ Eq. 8 x 10^{-2}	$H_K/\mu b^3$ Eq. 10 x 10^{-2}	$H_{PN}/\mu b^3$ Eq. 9 x 10^{-3}
V	2.63	9.4	9.5	9.3	3.8	3.9	4.2	1.9
Nb	2.86	9.5	10.7	9.3	3.8	4.4	4.5	2.4
Ta	2.86	16.6	8.9	9.3	3.8	3.6	5.5	1.6
Cr	2.50	17.6	7.8	8.5	3.3	3.1	3.7	1.2
Mo	2.73	25.5	7.6	8.3	3.3	3.0	4.1	1.1
W	2.73	31.5	8.4	8.2	3.2	3.2	4.1	1.3
Fe	2.48	11.2	7.8	8.3	3.4	3.2	2.7	1.3

†The value of μ is that given in Table II.

TABLE VII

Values of w and ℓ^* derived from the experimental data.

Metal	w/b	ℓ^*/b	
		Eq. 12	Eq. 12a
V	8	15	14
Nb	8	15	12
Ta	9	17	13
Cr	10	19	20
Mo	11	21	20
W	10	21	18
Fe	10	18	19

TABLE VIII

Effect of Strain on the Dislocation Density Participating in the Plastic Flow of Iron Determined from the Frequency Factor ν (After Conrad and Frederick (8))

Material	Strain	ν (Sec^{-1})	ρ (cm^{-2})
Vac. Melt. Electrolytic Iron-W.Q. from 920°C	1×10^{-3}	2.1×10^{7}	8.4×10^{8}
	5×10^{-2}	8.2×10^{7}	3.3×10^{9}
Ferrovac - Decarb.	2×10^{-2}	3.8×10^{6}	1.5×10^{8}
	10×10^{-2}	1.7×10^{8}	6.6×10^{9}
	20×10^{-2}	5.3×10^{9}	2.1×10^{11}
Ferrovac - Annealed	$>5 \times 10^{-2}$	5.3×10^{9}	2.1×10^{11}

References

1. A. H. Cottrell - Rept. on the Strength of Solids, Phys. Soc., London, p. 30 (1948); Conf. on High Rates of Strain, Inst. Mech. Eng. London p. 448 (1957); Trans. AIME 212 192 (1958).
2. A. H. Cottrell and B. A. Bilby - Proc. Phys. Soc. 62A 49 (1949).
3. J. C. Fisher - Trans. ASM 47 451 (1955).
4. N. F. Louat - Proc. Phys. Soc. B69 454 (1956); ibid B71 444 (1958).
5. Z. S. Basinski and J. W. Christian - Aust. J. Phys. 13 299 (1960).
6. H. Conrad - J. Iron and Steel Inst. 198 364 (1961).
7. J. W. Christian and B. C. Masters - private communication; Rept. entitled "Thermally-activated Flow in Body-Centered Cubic Metals" Res. Contract 7/Exptl/729, Nov. (1961).
8. H. Conrad and S. Frederick - Acta Met. 10 1013 (1962).
9. H. Conrad and W. Hayes - to be published in Trans. ASM.
10. J. Heslop and N. J. Petch - Phil. Mag. 1 866 (1956).
11. G. Schoeck - Acta Met. 9 382 (1961).
12. R. M. Rose, D. P. Ferris and J. Wulff - Trans. AIME 224 981 (1962).
13. B. L. Mordike - Zeit. f. Metall. 53 586 (1962).
14. B. L. Mordike and P. Haasen - Phil. Mag. 7 459 (1962).
15. N. Brown and R. A. Ekvall - Acta Met. 10 1101 (1962).
16. H. Conrad - "Yielding and Flow of Iron" to be published in AIME/Interscience-Wiley Vol. "High Purity Iron and Its Dilute Solid Solutions."
17. G. A. Sargent and A. A. Johnson - private communication; Rept. entitled "The Effects of Strain Rate and Temperature on the Plastic Deformation of Niobium"; also Fall Meeting AIME, New York City, Oct. (1962).
18. P. J. Sherwood - private communication; Rept. entitled "The Effect of Strain Rate on the Tensile Properties of Polycrystalline Tantalum at Room Temperature."
19. H. Schadler and J. R. Low - "Low-Temperature Brittleness of Refractory Metals," Contract No. Nonr-2614(00), Apr. (1962).
20. H. Conrad - Phil Mag. 5 745 (1960).
21. H. Conrad and G. Schoeck - Acta Met. 8 791 (1960).
22. K. Kitajima - Rept. Res. Inst. of Appl. Mech., Kyushu Univ., Japan, No. 15 171 (1960).
23. F. de Kazinski, W. A. Backofen, and B. Kapadia - "Fracture," Wiley p. 65 (1959).
24. N. J. Petch - "Fracture," Wiley p. 54 (1959).
25. W. Owen - AIME Refractory Metals Symposium, Chicago, Apr. 1962.
26. D. V. Wilson and B. Russel - Acta Met. 8 36 (1960).
27. E. O. Hall - Proc. Phys. Soc. B64 747 (1951).
28. N. J. Petch - J. Iron and Steel Inst. 174 25 (1953).
29. H. Conrad - to be published in Acta Met. and in AIME-Interscience Vol. on Recovery and Recrystallization.
30. T. Tietz and J. Wilson - "Mechanical, Oxidation, and Thermal Property Data for Seven Refractory Metals and Their Alloys" - Lockheed Missiles and Space Div. Rept. Code 2-36-61-1, Sept. 15, 1961.
31. D. S. Clark and D. S. Wood - Proc. ASTM 49 717 (1949); Trans. ASM 43 571 (1951); ibid 44 726 (1952); ibid 46 34 (1954).
32. J. M. Kraft and A. M. Sullivan - Trans. ASM 51 643 (1959).
33. H. Conrad and H. Wiedersich - Acta Met. 8 128 (1960).

34. C. Zener and J. H. Hollomon - J. Appl. Phys. 15 22 (1944).
35. T. Yokobori - Phys. Rev. 88 1423 (1952).
36. J. D. Campbell - Acta Met. 1 706 (1953); Trans. ASM 51 659 (1959).
37. A. W. Magnusson and W. M. Baldwin - J. Mech. & Phys. Solids 5 172 (1957).
38. J. B. Lean, J. Plateau and C. Crussard - Mem. Sci. Revise Metall. 56 427 (1959).
39. R. Chambers - Fall Meeting AIME, New York, Oct. (1962).
40. A. H. Cottrell - Trans. AIME 212 192 (1958).
41. J. R. Low and R. W. Guard - Acta Met. 7 171 (1959).
42. A. Keh and S. Weissmann - Conference on the Impact of Transmission Electron Microscopy on Theories of the Strength of Crystals," Berkeley (1961); to be published by Interscience.
43. D. P. Gregory and G. H. Rowe - "Mechanism of Work Hardening in B.C.C. Metals," PWAC-375, ASD Rept. TRD-62-354, July 12, 1962.
44. A. Seeger - Phil Mag. 1 651 (1956).
45. A. Seeger, H. Donth and F. Pfaff - Disc. Faraday Soc. 23 19 (1957).
46. A. H. Cottrell - "Dislocations and Plastic Flow in Crystals," Oxford Press (1953) p. 62.
47. D. Kuhlmann-Wilsdorf - Phys. Rev. 120 773 (1960).
48. R. Hobart and V. Celli - J. Appl. Phys. 33 60 (1962).
49. A. Seeger and P. Schiller - Acta Met. 10 348 (1962).
50. D. F. Stein and J. R. Low - J. Appl. Phys. 31 362 (1960).
51. W. C. Leslie - Acta Met. 9 1004 (1961).
52. L. I. Van Torne and G. Thomas - submitted to Acta Met.
53. A. Brailsford - Phys. Rev. 122 778 (1961).
54. R. Chambers - private communication.
55. J. S. Koehler - Phys. Rev. 86 52 (1952).
56. E. Orowan - "Dislocations in Metals," AIME, New York, p. 103 (1954).
57. W. G. Johnston and J. J. Gilman - J. Appl. Phys. 30 129 (1959); ibid 31 632 (1960).
58. R. Benson - private communication.

Sources of Data other than those Referenced in the Text

59. T. A. Trozera, O. D. Sherby and J. E. Dorn - Trans. ASM 49 173 (1957).
60. R. P. Carreker and W. R. Hibbard - Acta Met. 1 654 (1953).
61. J. H. Bechtold and P. G. Shewmon - Trans. ASM 46 397 (1954).
62. J. H. Bechtold - Trans. AIME 206 142 (1956).
63. J. W. Pugh - Proc. ASTM 57 906 (1957).
64. Metals Res. Labs, Union Carbide Co., "Investigation of the Properties of Tungsten and Its Alloys" WADD Tech Rept 60-144, May (1960).
65. H. G. Sell et al - "The Physical Metallurgy of Tungsten and Tungsten Base Alloys" Contract No. AF 33(616)-6933, Proj. No. 735101, Jan 12, 1962.
66. E. S. Tankins and R. Maddin - "Columbium Metallurgy" Interscience New York, p. 343 (1961).
67. E. T. Wessel, L. L. France and R. T. Begley - "Columbium Metallurgy" Interscience, New York, P. 459 (1961).
68. M. A. Adams and A. Iannucci - "The Mechanical Properties of Tantalum with Special Reference to the Ductile-Brittle Transition," ASD Tech. Rept. 61-203, Apr. 1, 1961.
69. M. J. Marcinkowski and H. A. Lipsitt - Acta Met. 10 95 (1962).

70. R. W. Armstrong - "The Plastic Flow of Molybdenum from -200°C to +400°C by Compression Tests" - Westinghouse Res. Rept. 60-8-01-01-R3, Nov. 7 (1955).
71. J. A. Hendrickson, D. S. Wood, and D. S. Clark - Trans. ASM 48 540 (1956).
72. D. Weinstein, G. M. Sinclair and C. A. Wert - "The Strain Rate and Temperature Dependence of the Ductile-to-Brittle Transition in Molybdenum Subjected to Torsional Loading" - Univ. Ill. T. & A.M. Rept. No.156, Dec. (1959).
73. B. Jaoul and D. Gonzalez - J. Mech. Phys. Solids 9, 16 (1961).
74. R. Guard - Acta Met. 9 163 (1961).
75. J. H. Bechtold - Acta Met. 3 249 (1955).
76. J. W. Pugh - Trans. ASM 48 677 (1956).
77. P. E. Bennett and G. M. Sinclair - Univ. of Illinois T. & A.M. Rept.No. 157, Dec. (1959).

Sources of Data listed in the Figures

Fig. No.	References
2	7, 8, 59, 60
6	12, 19, 61-65
12	7, 9
13	7, 9, 66, 67
14	7, 9, 14, 68
15	9, 69
16	9, 70-72
17	9, 12, 19, 64
18	6, 14, 16, 50, 73, 74
21	7, 14, 18, 68, 75, 76
22	12, 19, 62-64
23	6, 14, 16, 50, 73, 74
25	31, 77

FIG. 1 INITIAL YIELD STRESS OF VARIOUS POLYCRYSTALLINE METALS VERSUS T/Tm

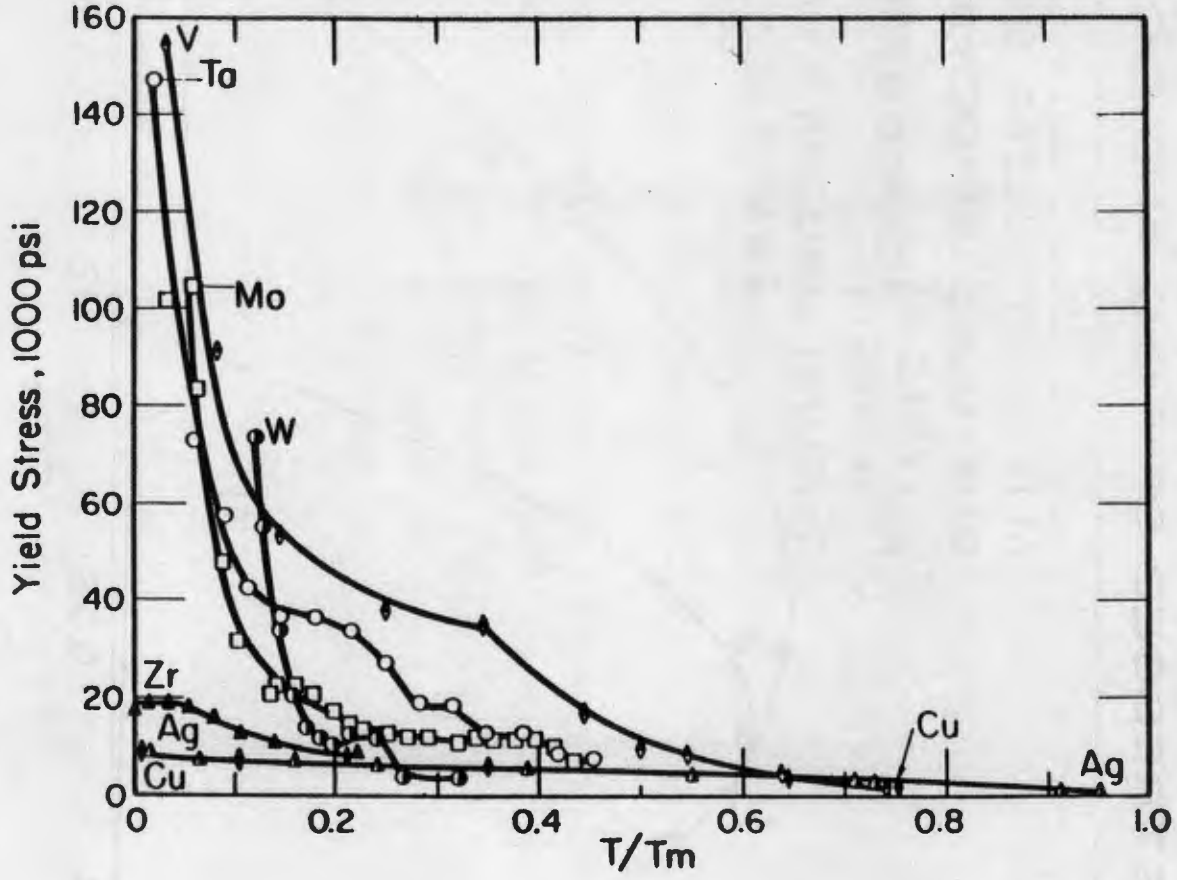

FIG. 2 EFFECT OF STRAIN RATE ON THE YIELD AND FLOW STRESSES OF F.C.C. AND B.C.C. METALS

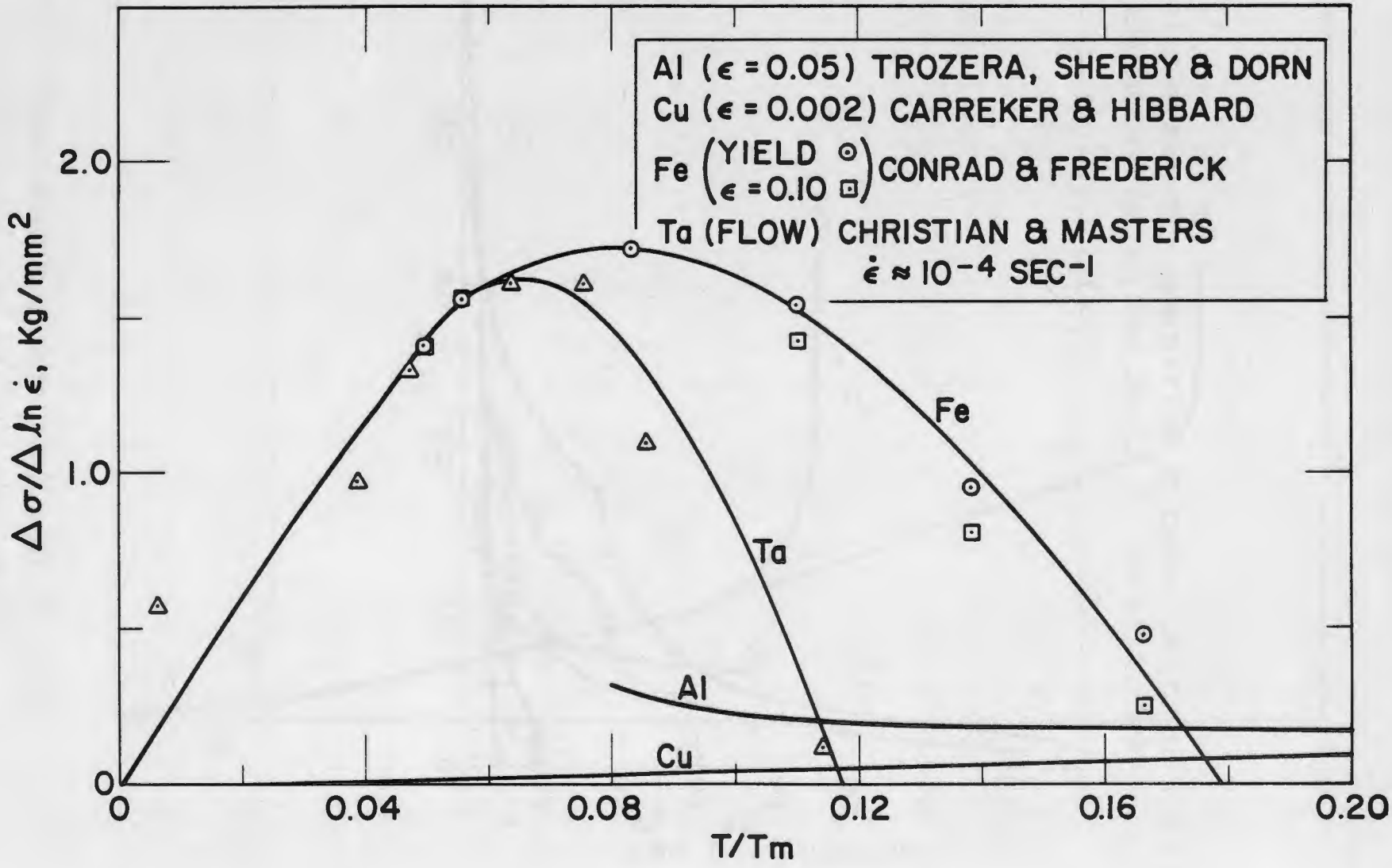

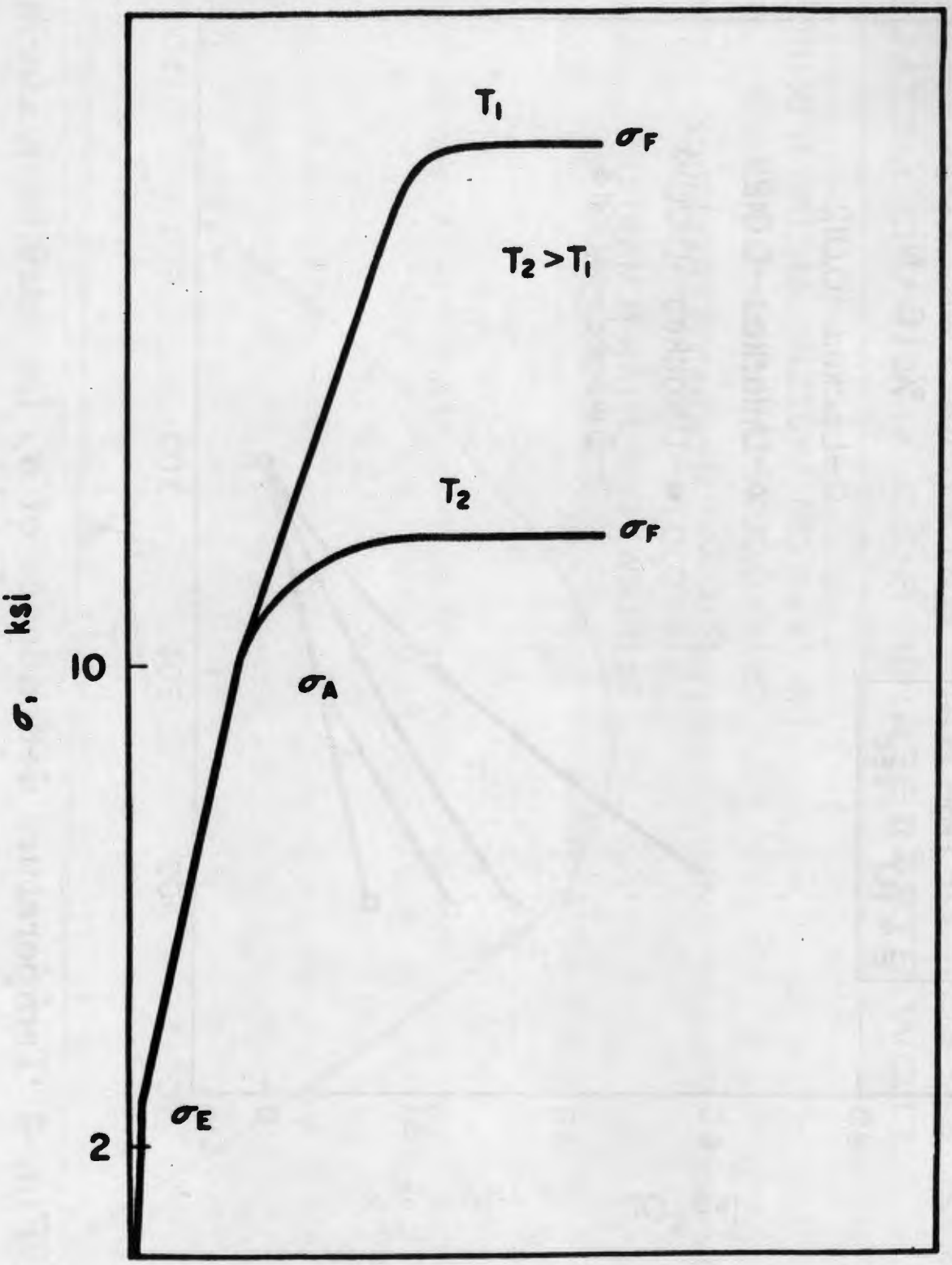

FIG. 3 Idealized stress–strain curves for an ultra-pure iron at two temperatures.
(AFTER BROWN AND EKVALL (15))

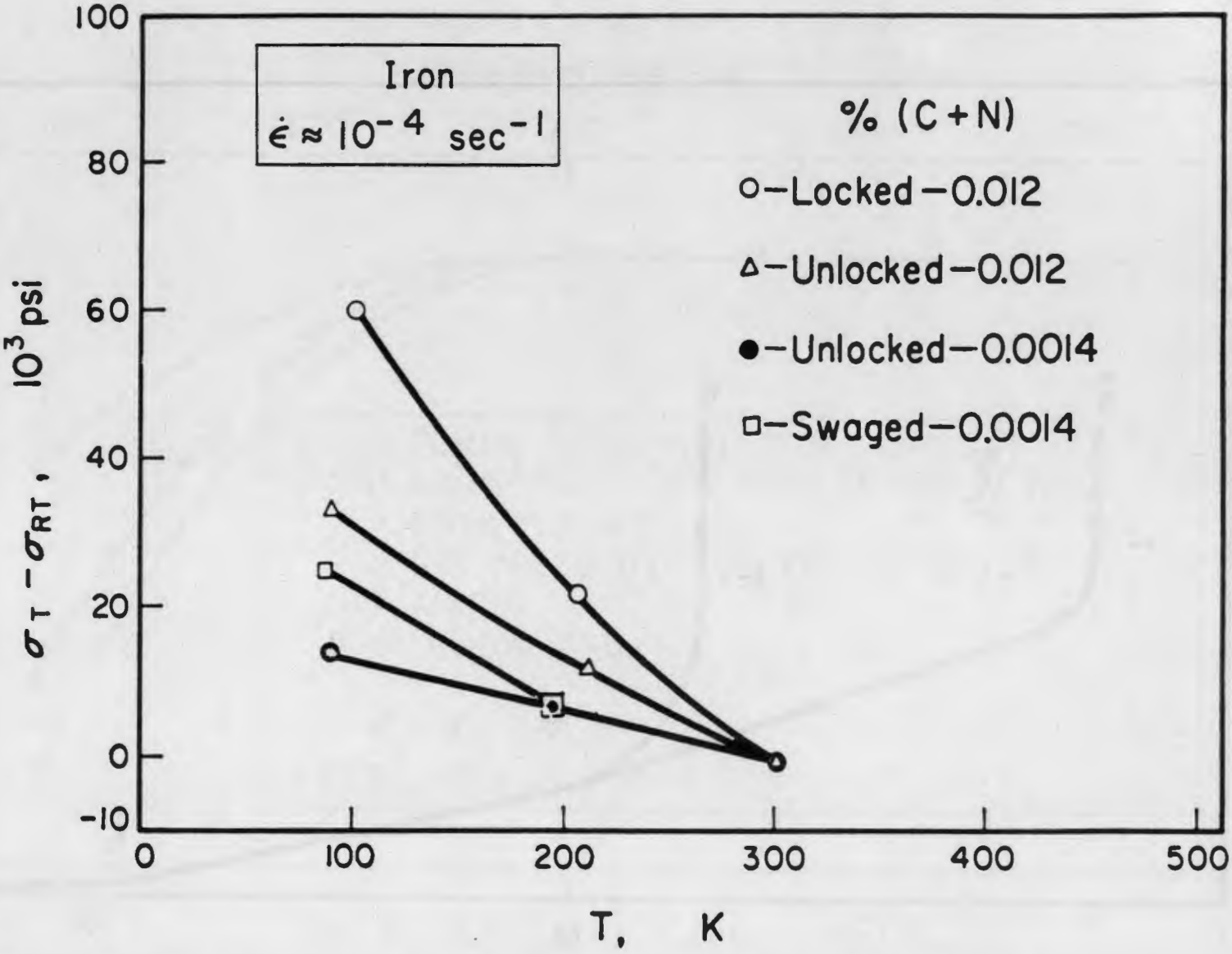

FIG. 4 Temperature dependence of σ_A for various materials and state of locking.
(AFTER BROWN AND EKVALL (15))

FIG. 5 EFFECT OF TEMPERATURE ON THE INITIAL YIELD STRESS, THE PROPORTIONAL LIMIT AFTER STRAINING AND THE FLOW STRESS OF ELECTROLYTIC IRON

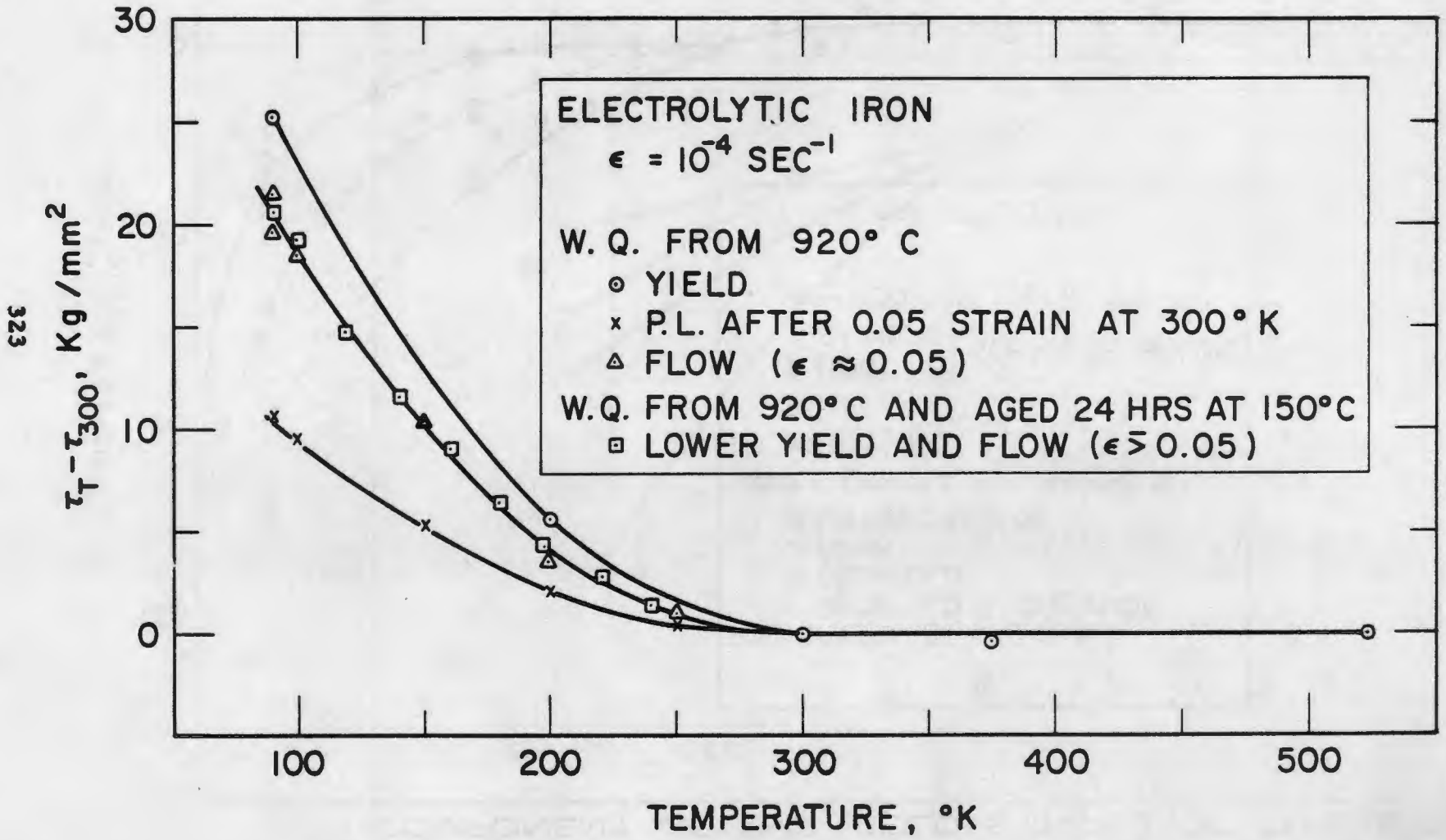

FIG. 6 EFFECT OF TEMPERATURE ON THE THERMAL COMPONENT OF THE YIELD STRESS OF TUNGSTEN

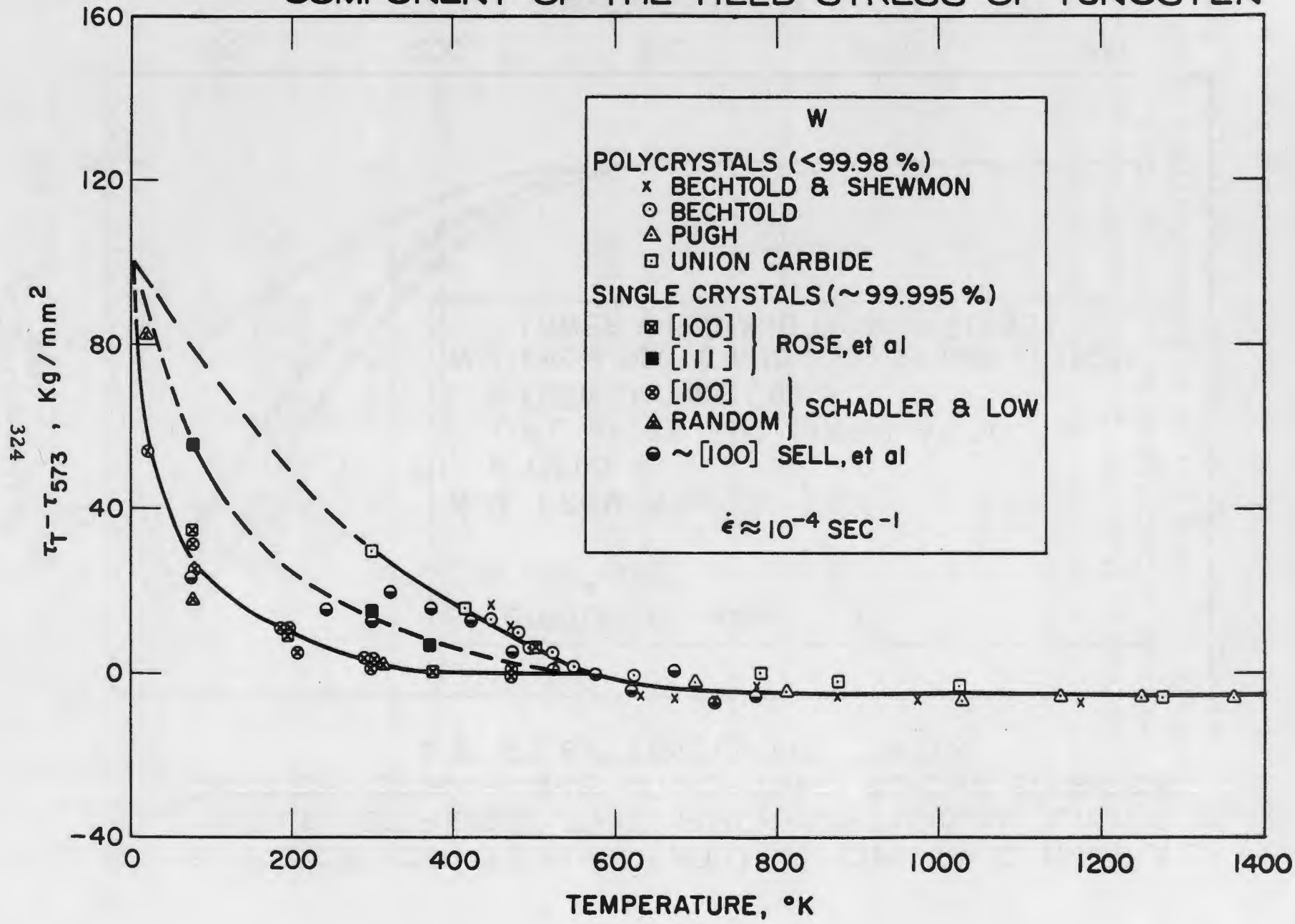

FIG. 7 VARIATION OF τ^* WITH TEMPERATURE FOR PURE (< 0.005 WT % INTERSTITIALS) AND IMPURE (> 0.02 WT % INTERSTITIALS) GROUP VA METALS. STRAIN RATE: 10^{-4} SEC^{-1}

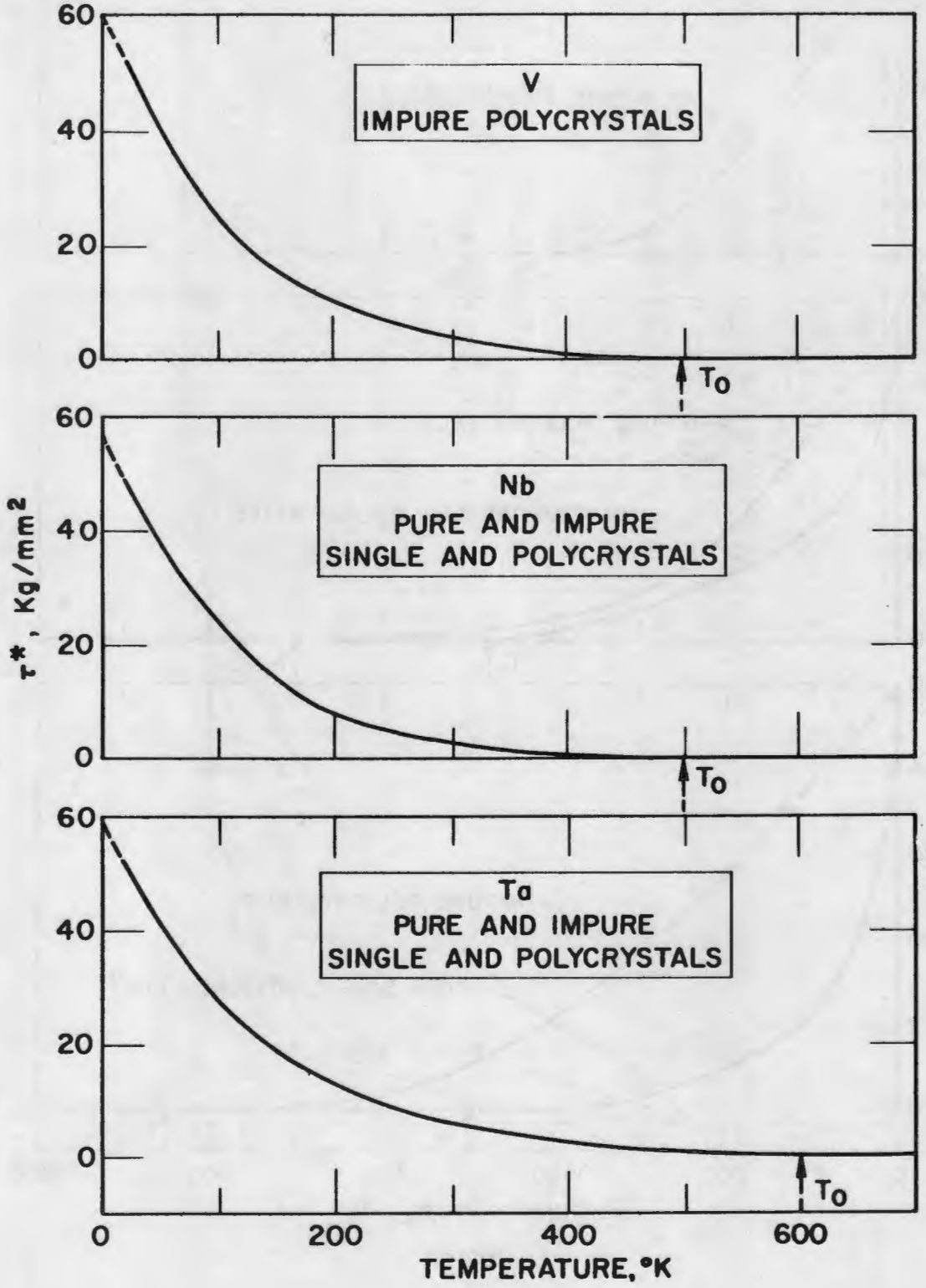

FIG. 8 VARIATION OF τ^* WITH TEMPERATURE FOR PURE (<0.005 WT % INTERSTITIALS) AND IMPURE (>0.02 WT % INTERSTITIALS) GROUP VIA METALS. STRAIN RATE: 10^{-4} SEC^{-1}

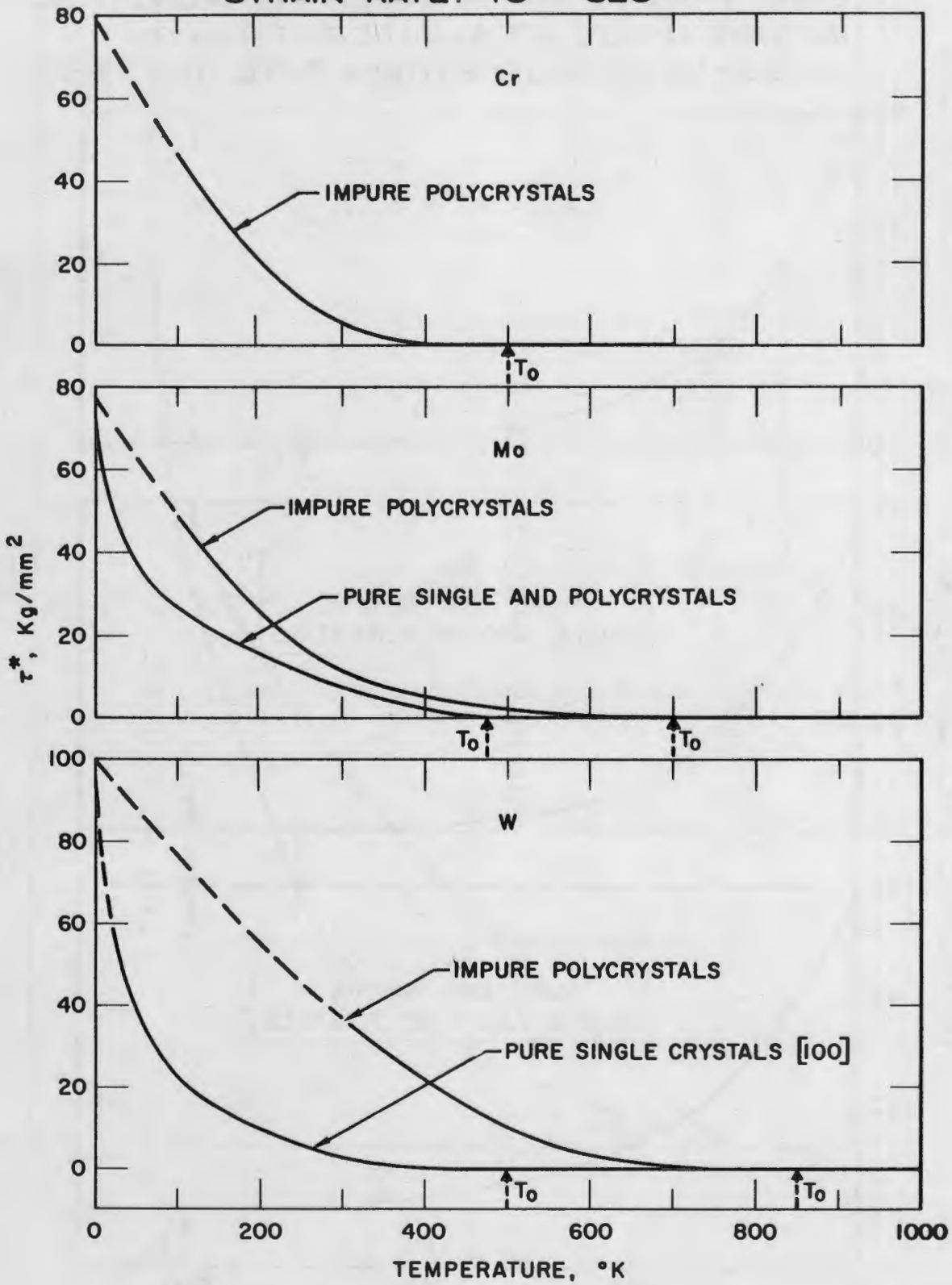

FIG. 9 VARIATION OF τ^* WITH TEMPERATURE FOR PURE (<0.005 WT% INTERSTITIALS) AND IMPURE (>0.02 WT% INTERSTITIALS) IRON

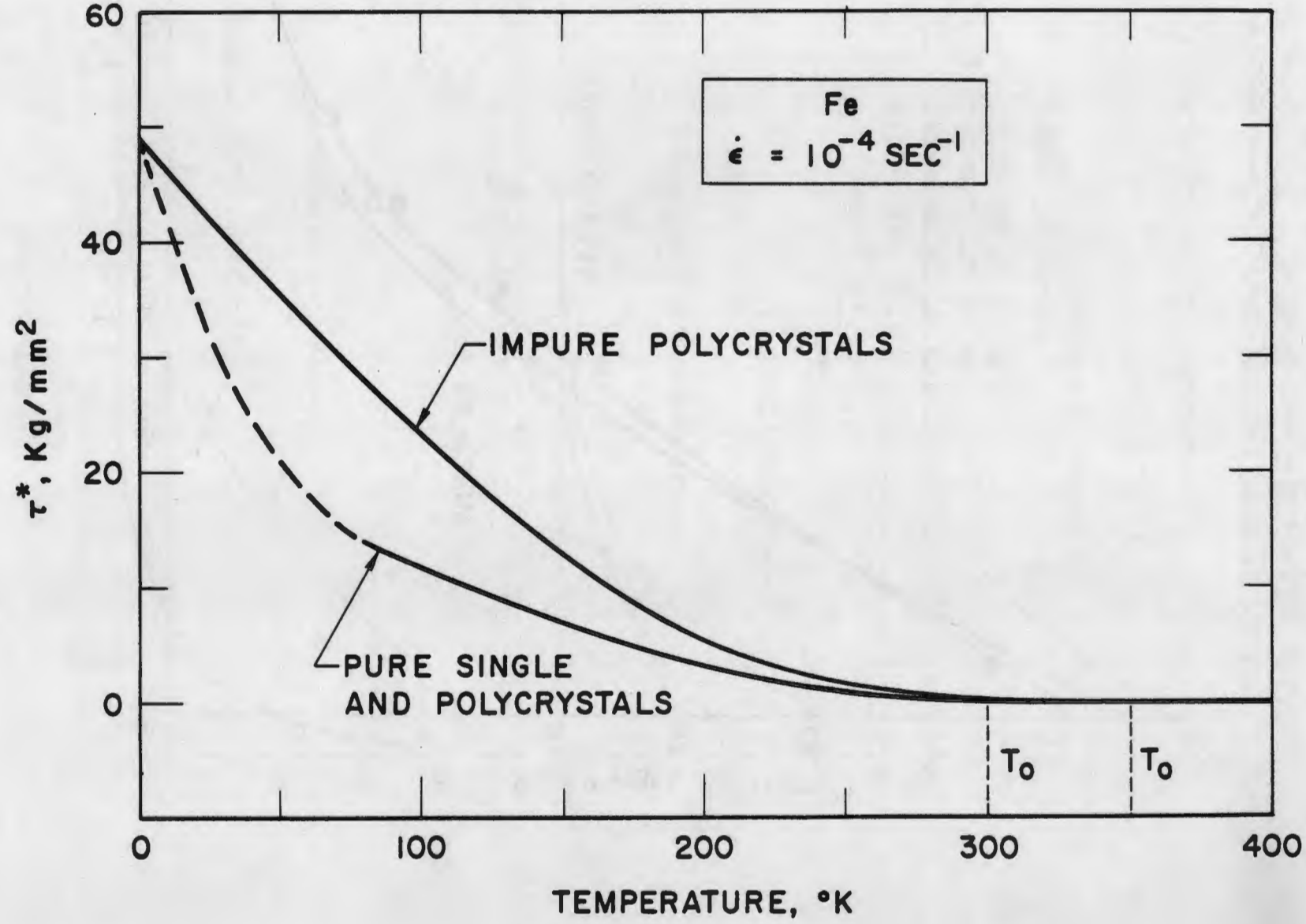

FIG. 10 TEMPERATURE DEPENDENCE OF REVERSIBLE FLOW STRESS IN IRON [AFTER BAZINSKI AND CHRISTIAN (5)]

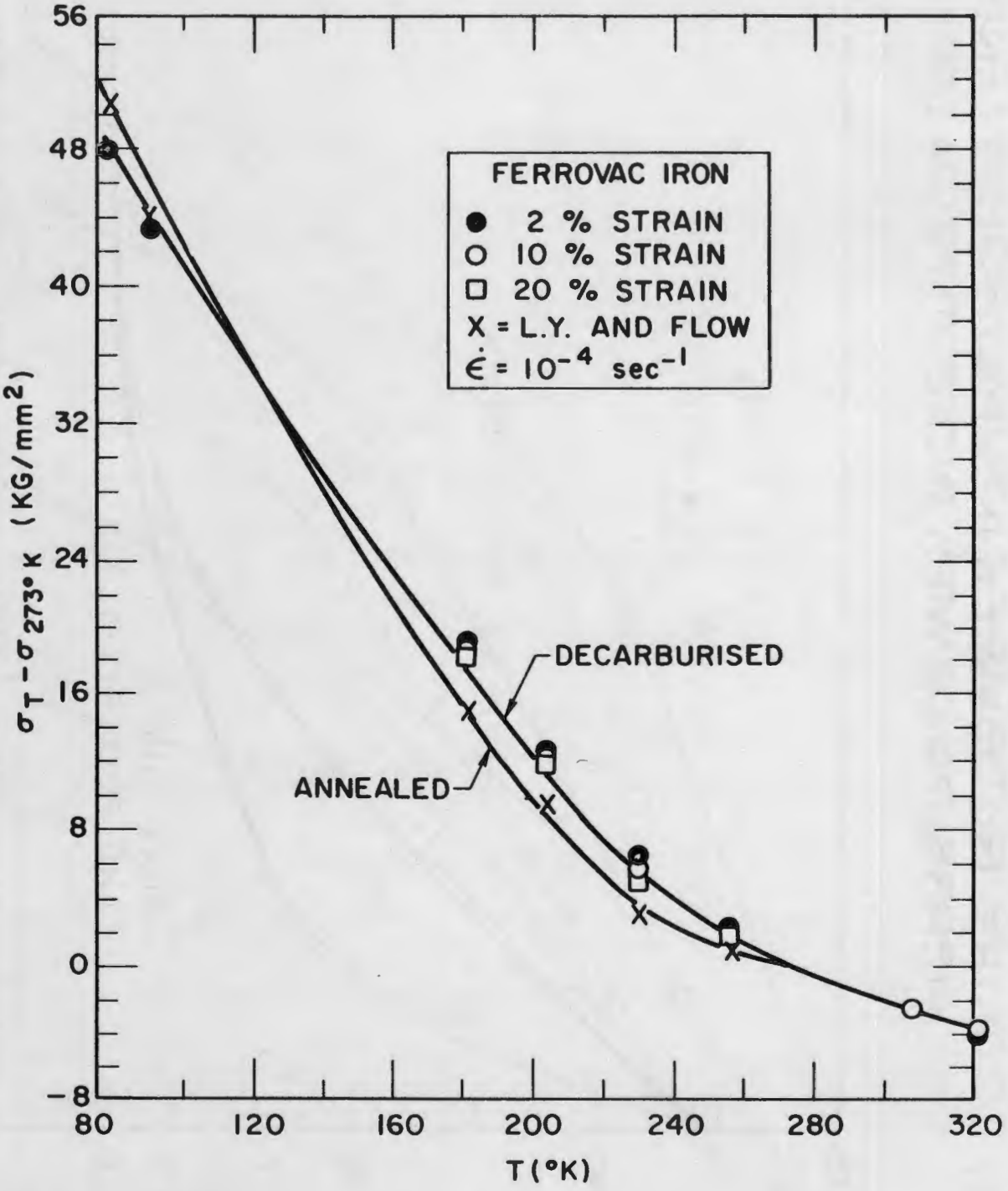

FIG. 11. LOG τ^* VS TEMPERATURE FOR IMPURE POLYCRYSTALLINE B.C.C. METALS

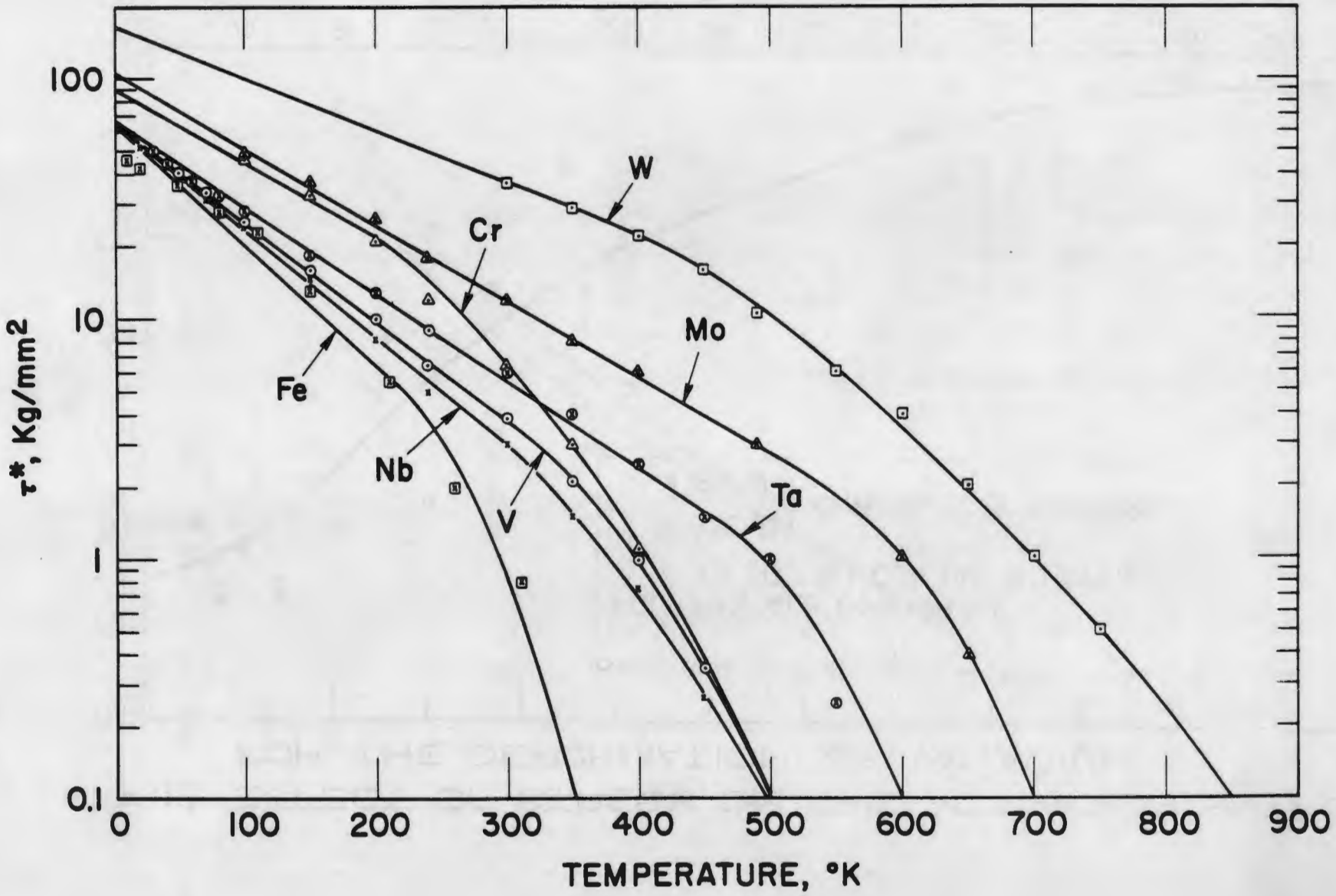

FIG. 12 EFFECT OF STRESS ON THE ACTIVATION ENERGY FOR THE DEFORMATION OF VANADIUM

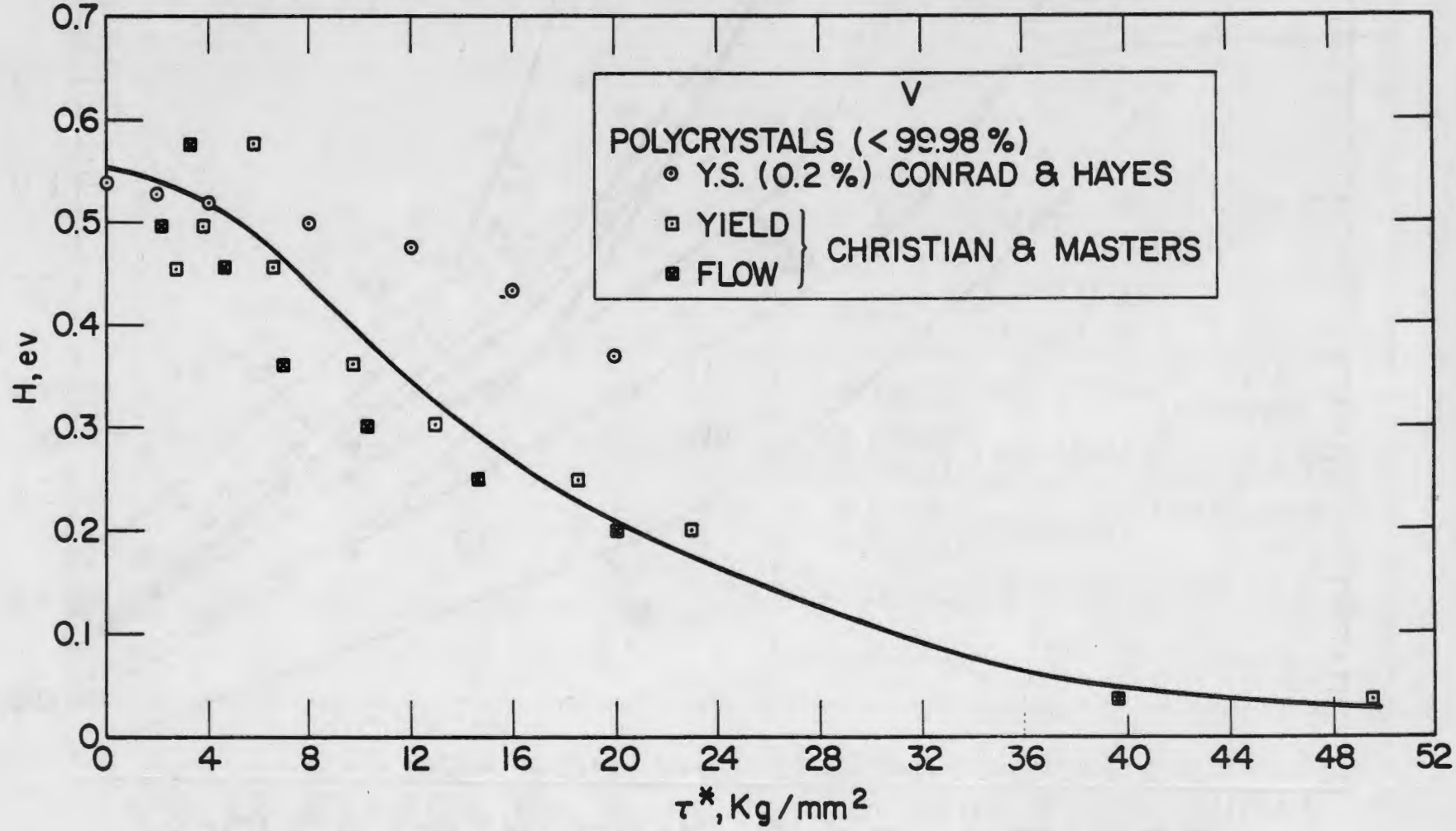

FIG. 13 EFFECT OF STRESS ON THE ACTIVATION ENERGY FOR THE DEFORMATION OF NIOBIUM

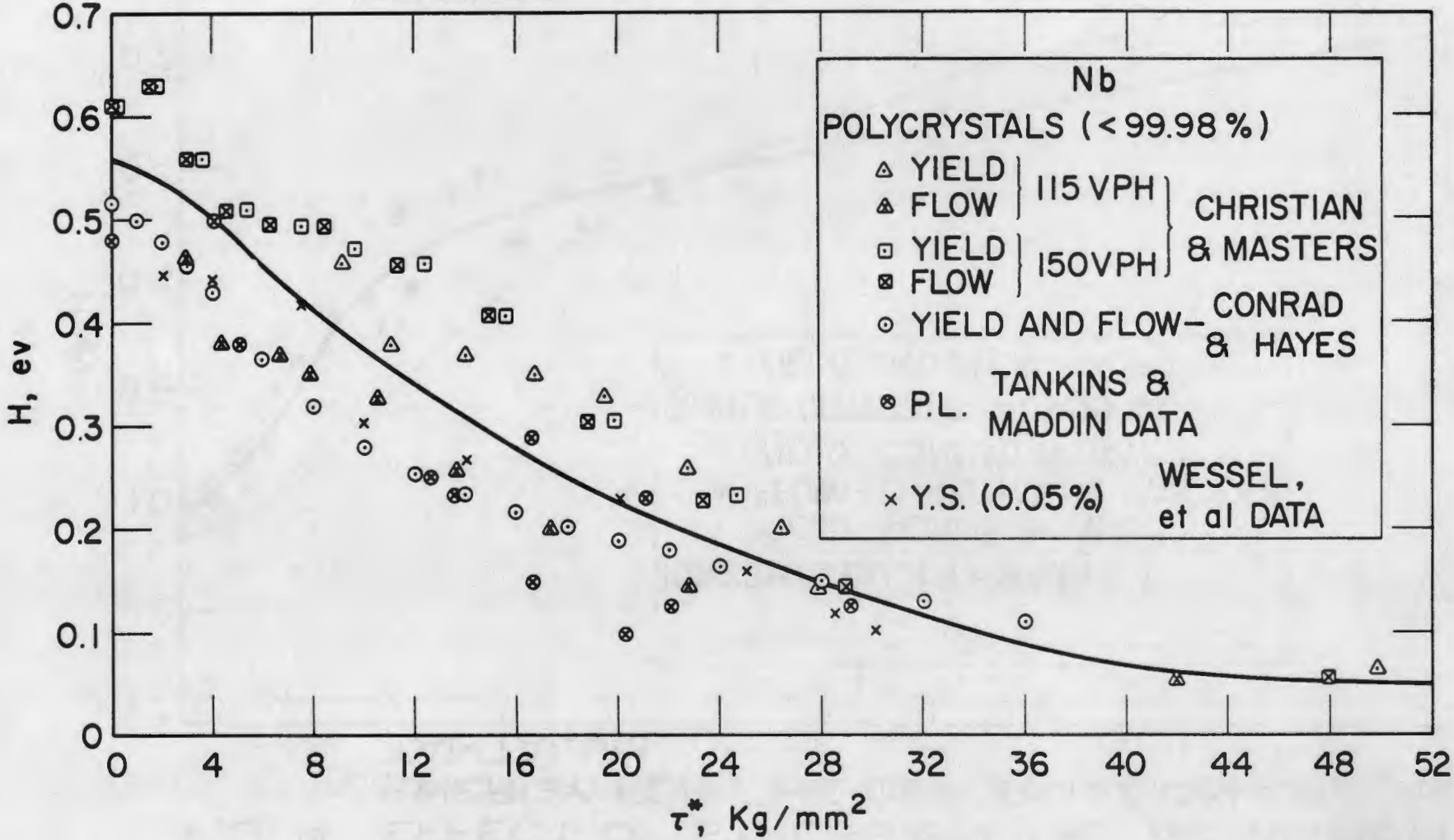

FIG. 14· EFFECT OF STRESS ON THE ACTIVATION ENERGY FOR THE DEFORMATION OF TANTALUM

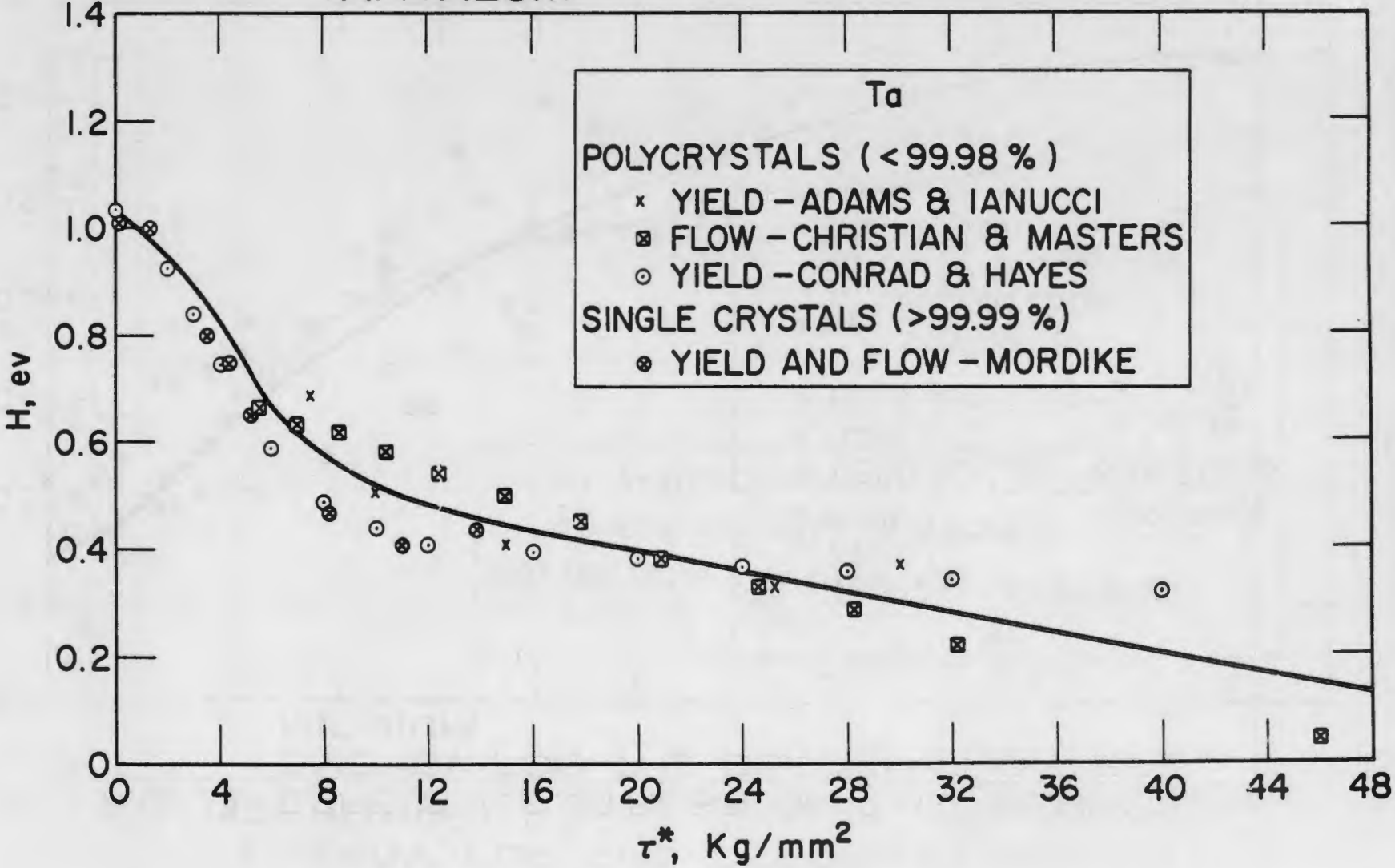

FIG. 15 EFFECT OF STRESS ON THE ACTIVATION ENERGY FOR THE DEFORMATION OF CHROMIUM

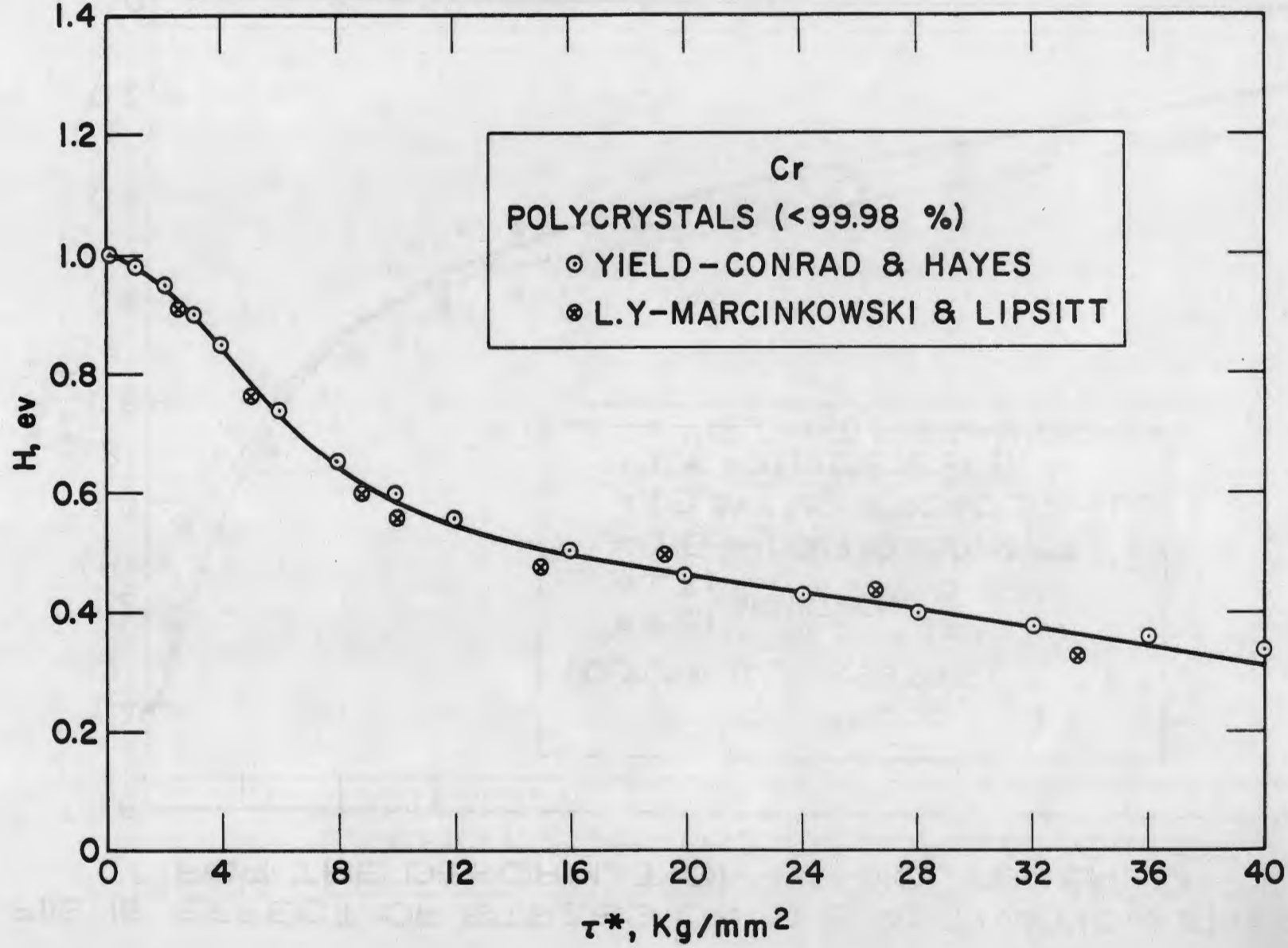

FIG. 16 EFFECT OF STRESS ON THE ACTIVATION ENERGY FOR THE DEFORMATION OF MOLYBDENUM

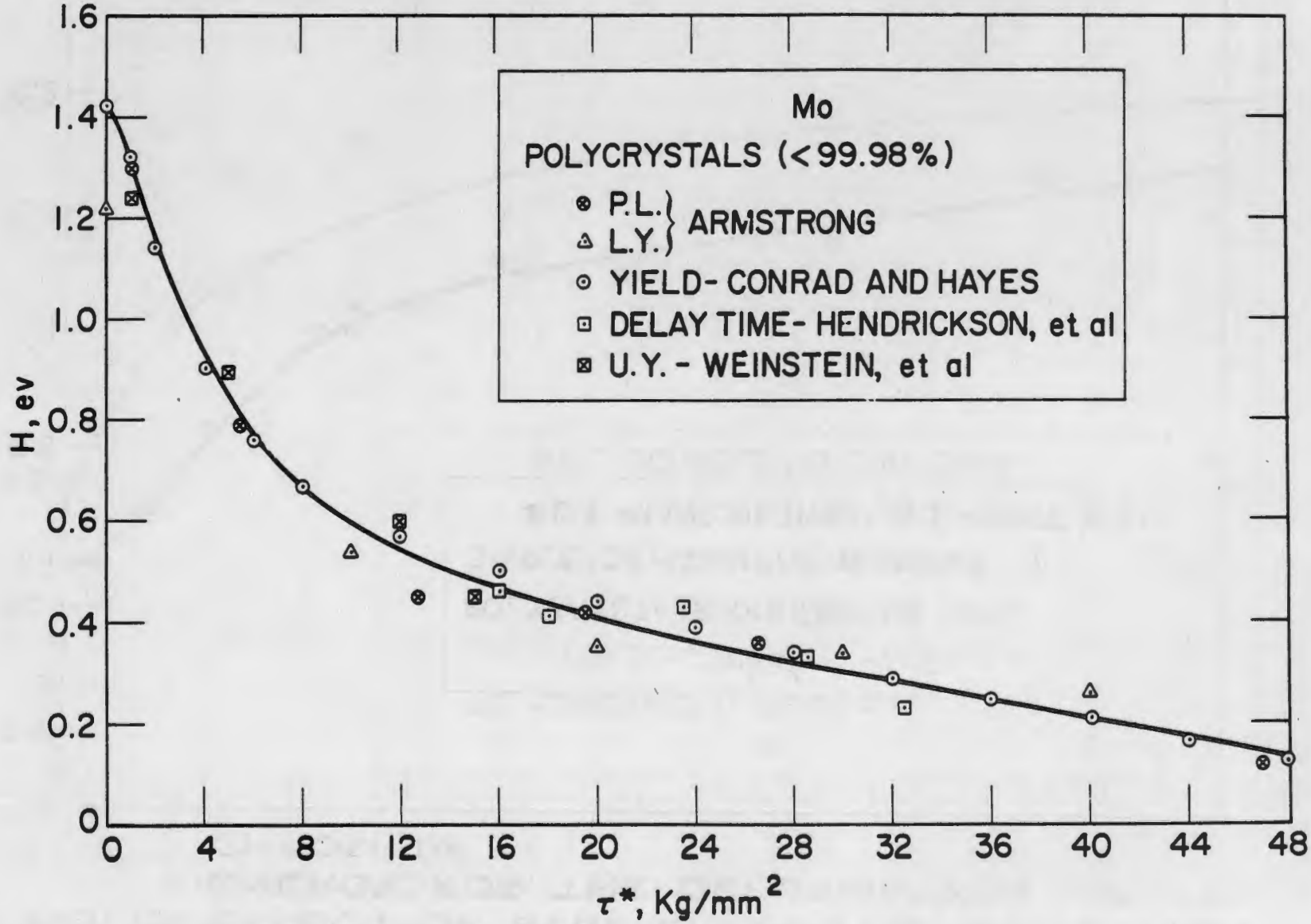

FIG. 17- EFFECT OF STRESS ON THE ACTIVATION ENERGY FOR THE DEFORMATION OF TUNGSTEN

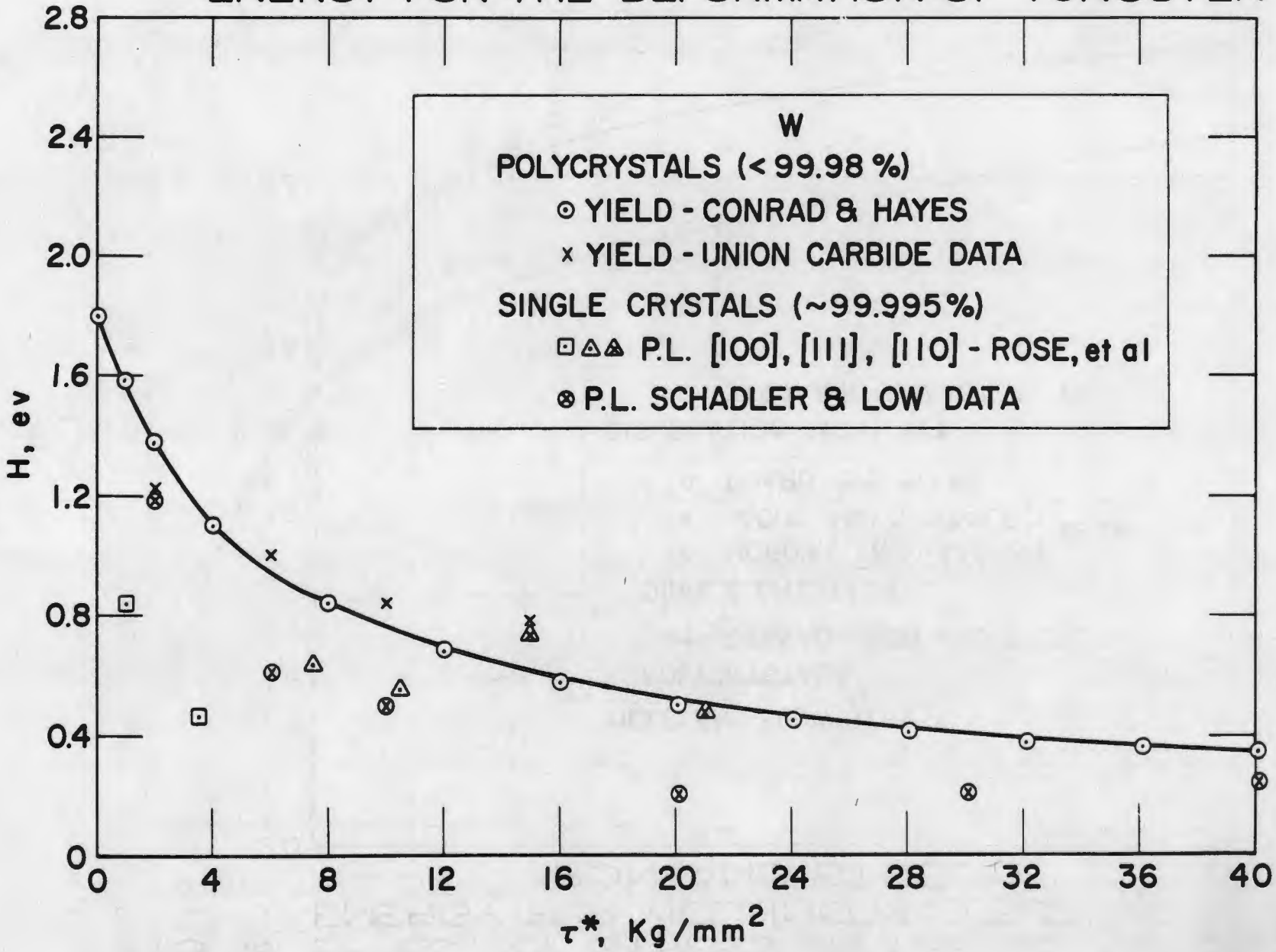

FIG. 18 EFFECT OF STRESS ON THE ACTIVATION ENERGY FOR YIELDING AND FLOW IN IRON AND STEEL

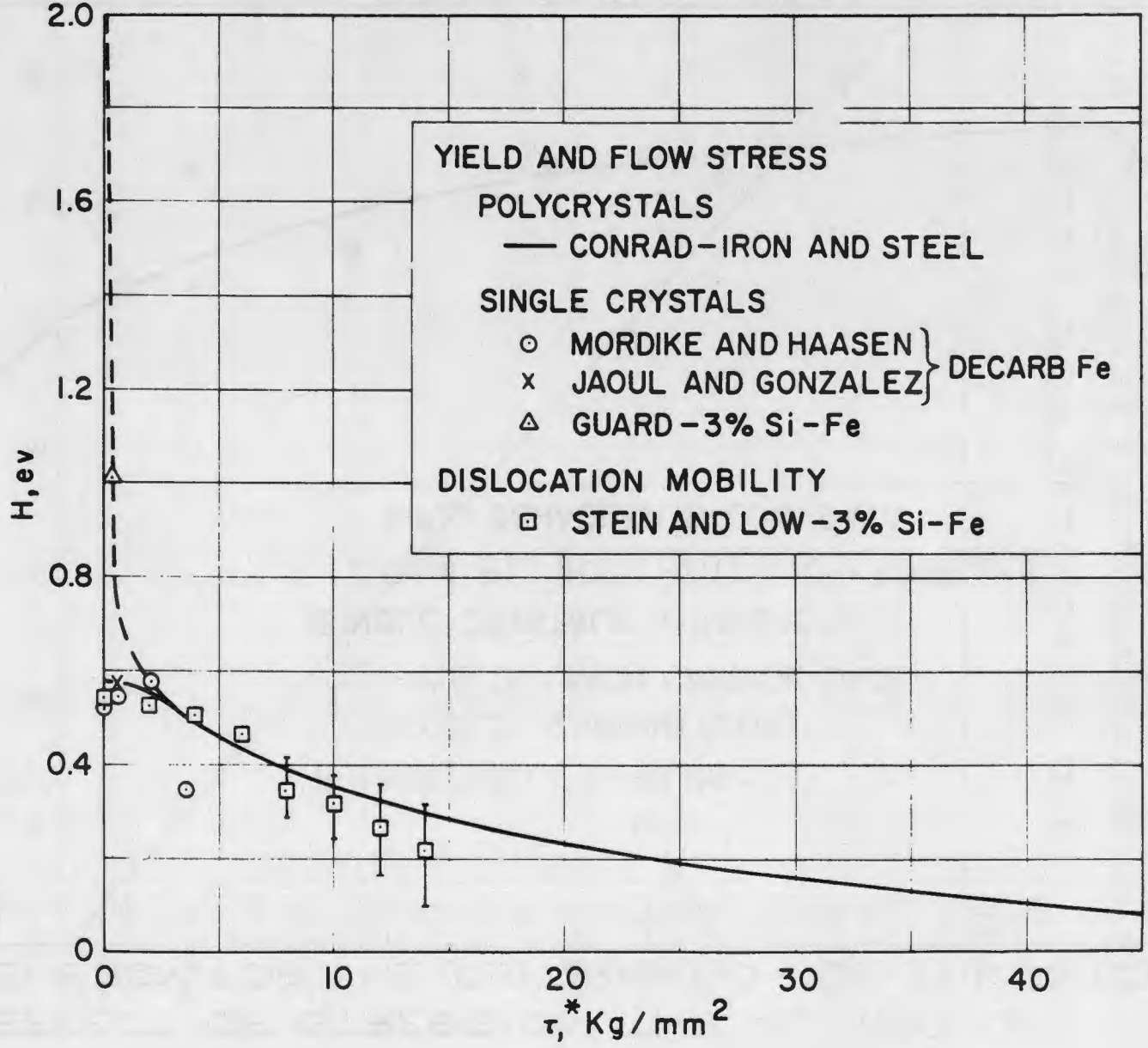

FIG. 19. RELATIONSHIP BETWEEN $H_o(\tau^* = 1 Kg/mm^2)$ AND μb^3 FOR THE B.C.C. METALS

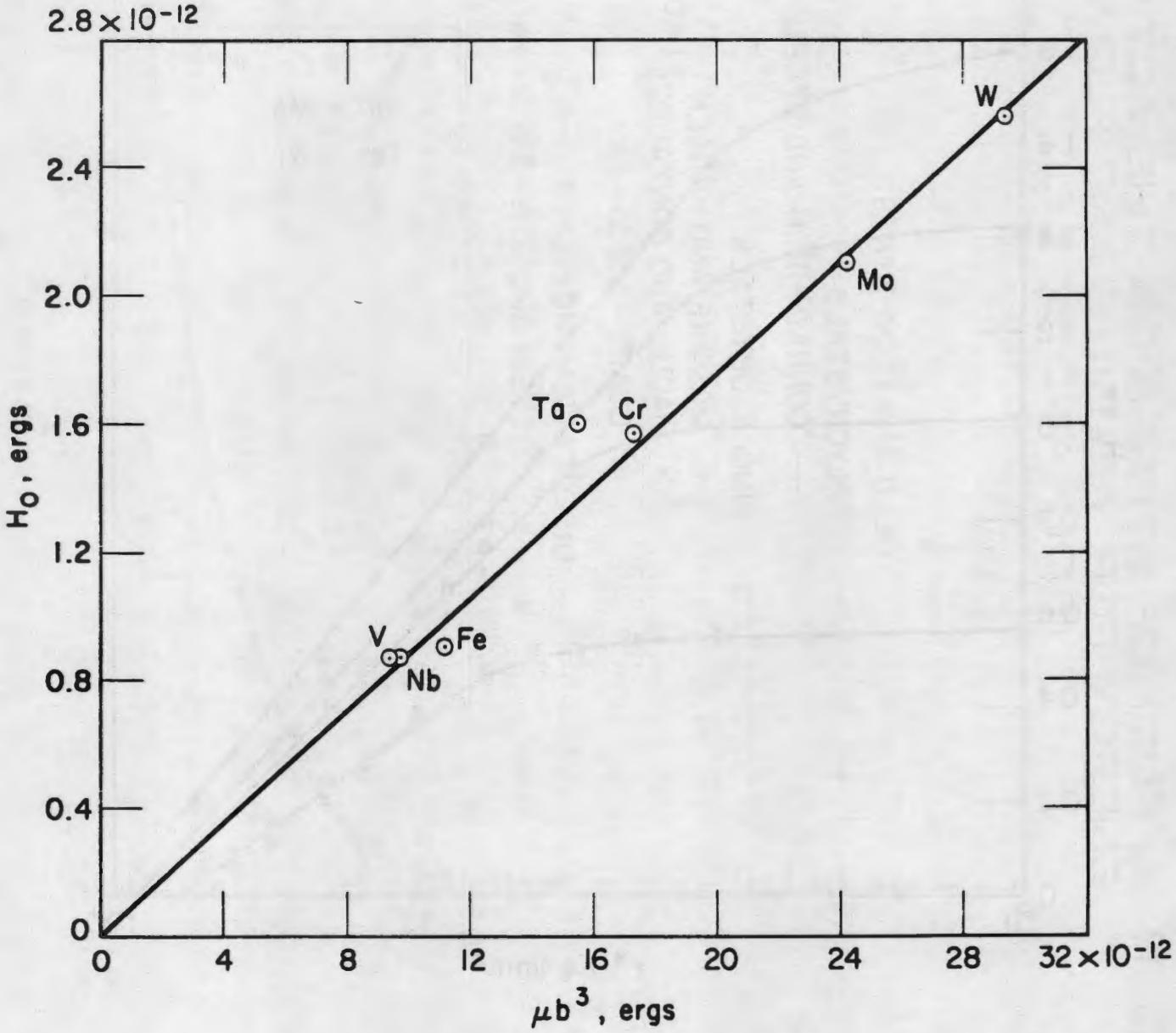

FIG. 20. ACTIVATION ENERGY VS LOG τ^* FOR THE B.C.C. METALS

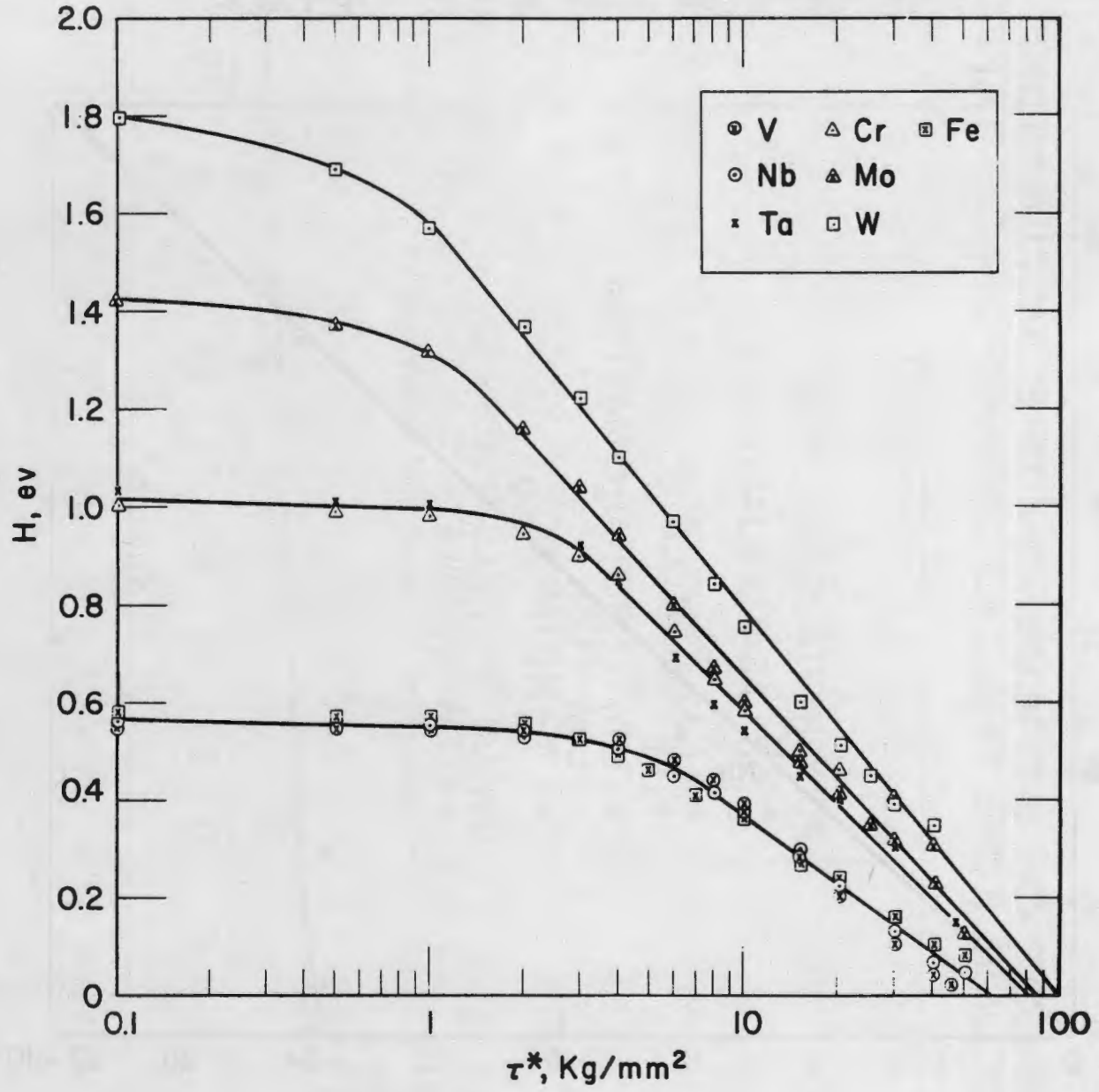

FIG. 21 EFFECT OF STRESS ON THE ACTIVATION VOLUME FOR THE DEFORMATION OF TANTALUM

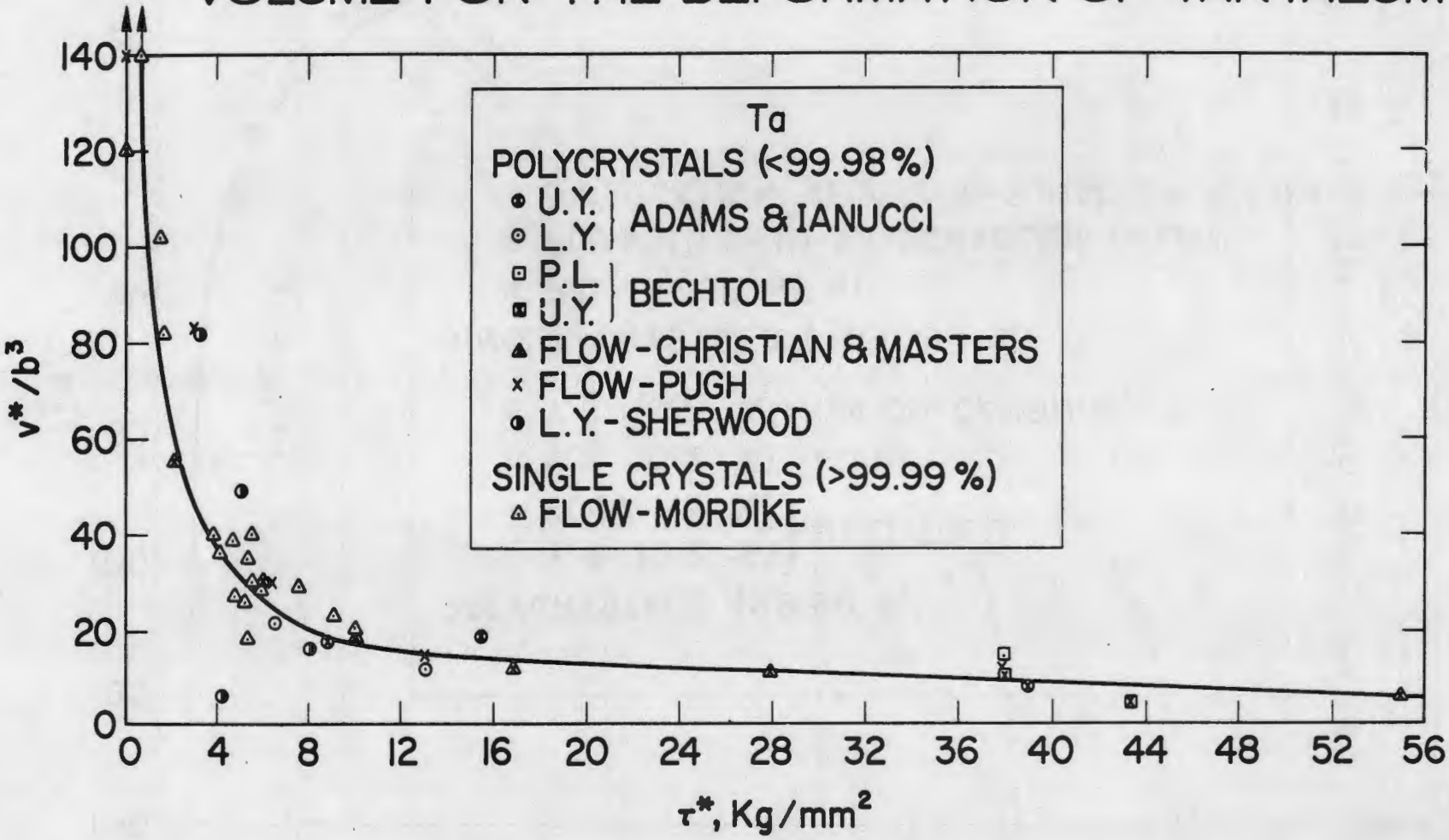

FIG. 22 EFFECT OF STRESS ON THE ACTIVATION VOLUME FOR THE DEFORMATION OF TUNGSTEN

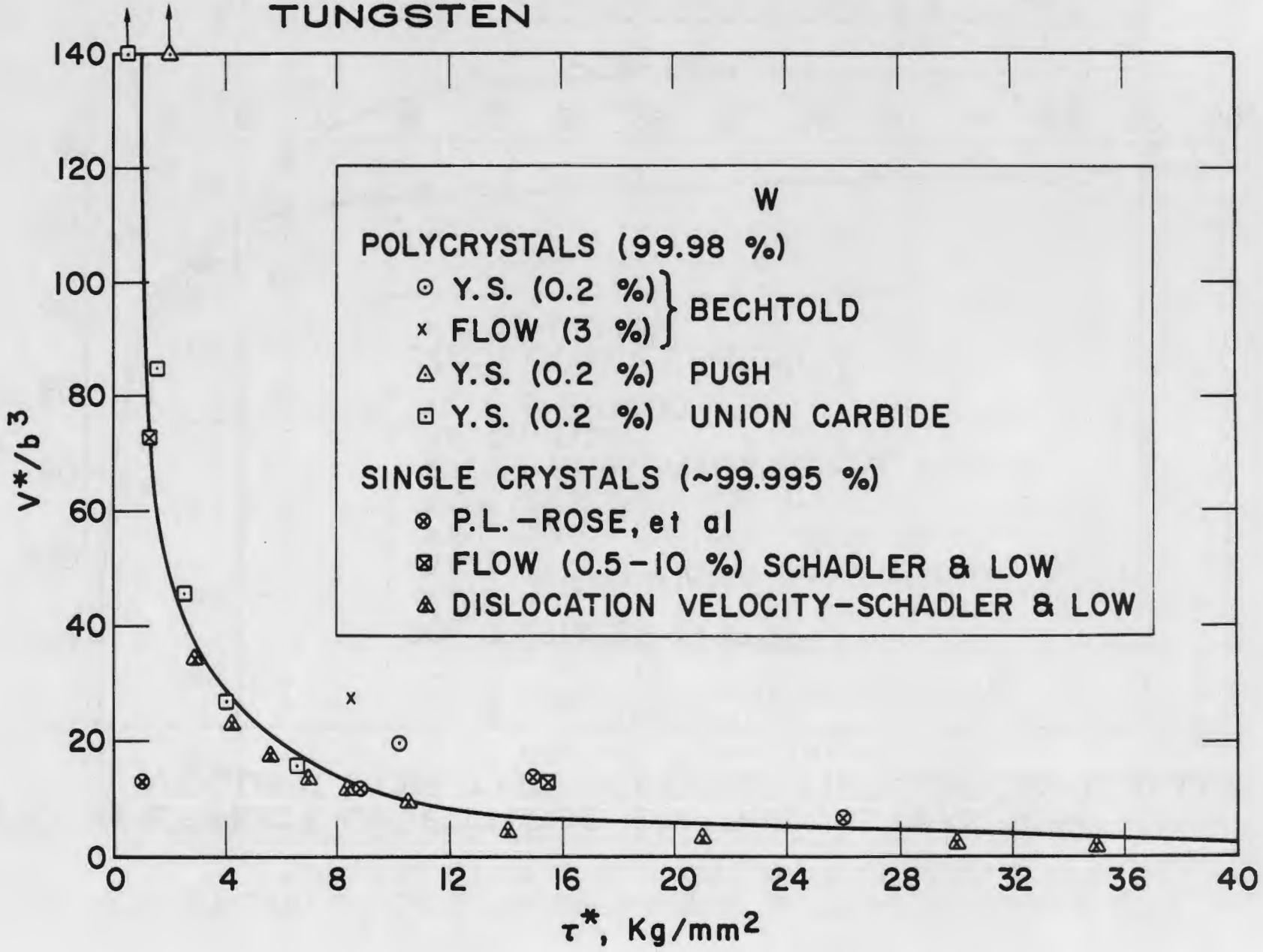

FIG. 23 EFFECT OF STRESS ON THE ACTIVATION VOLUME FOR YIELDING AND FLOW IN IRON AND STEEL

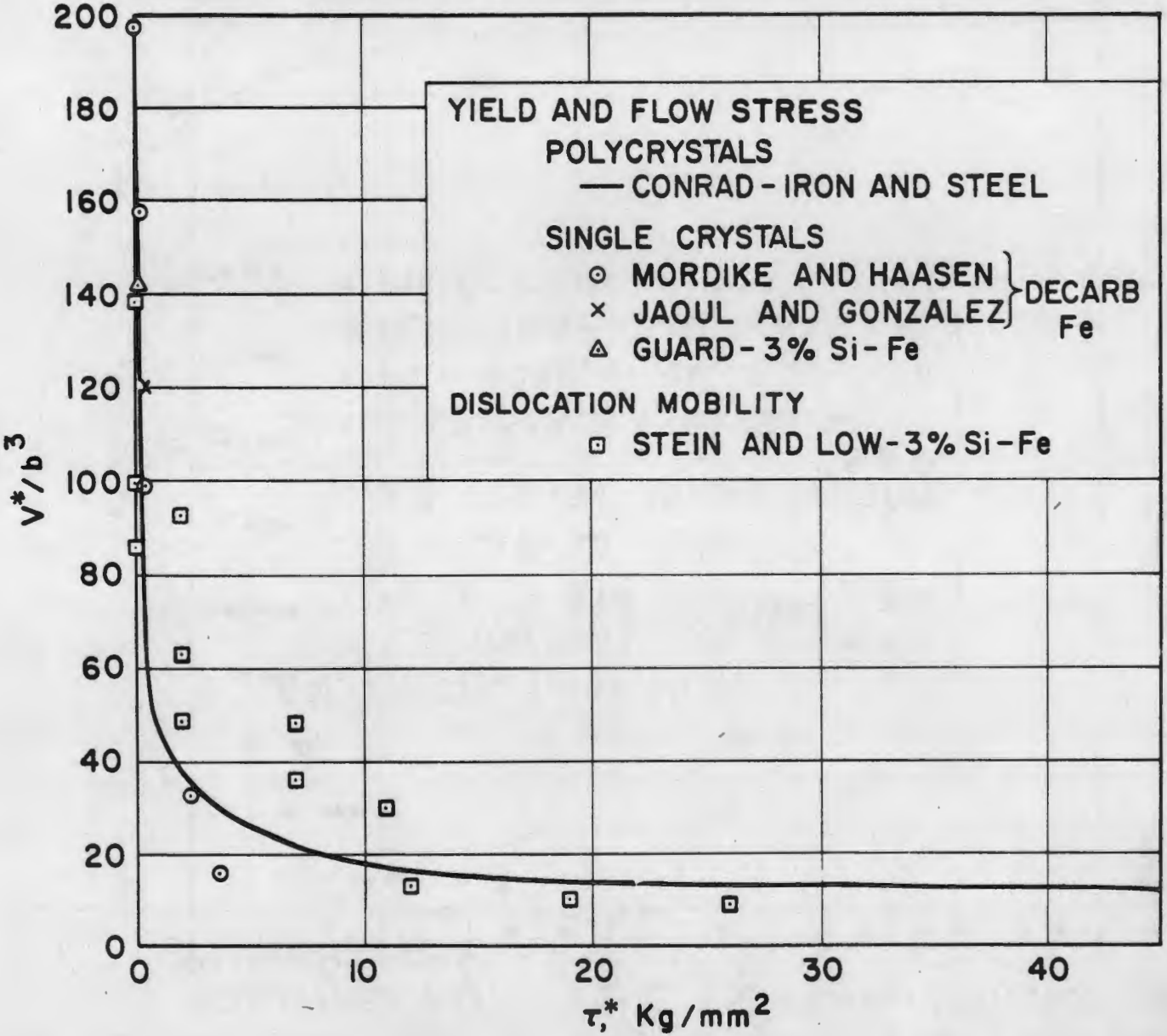

FIG. 24 EFFECT OF STRESS ON THE ACTIVATION VOLUME FOR DEFORMATION OF THE B.C.C. TRANSITION METALS

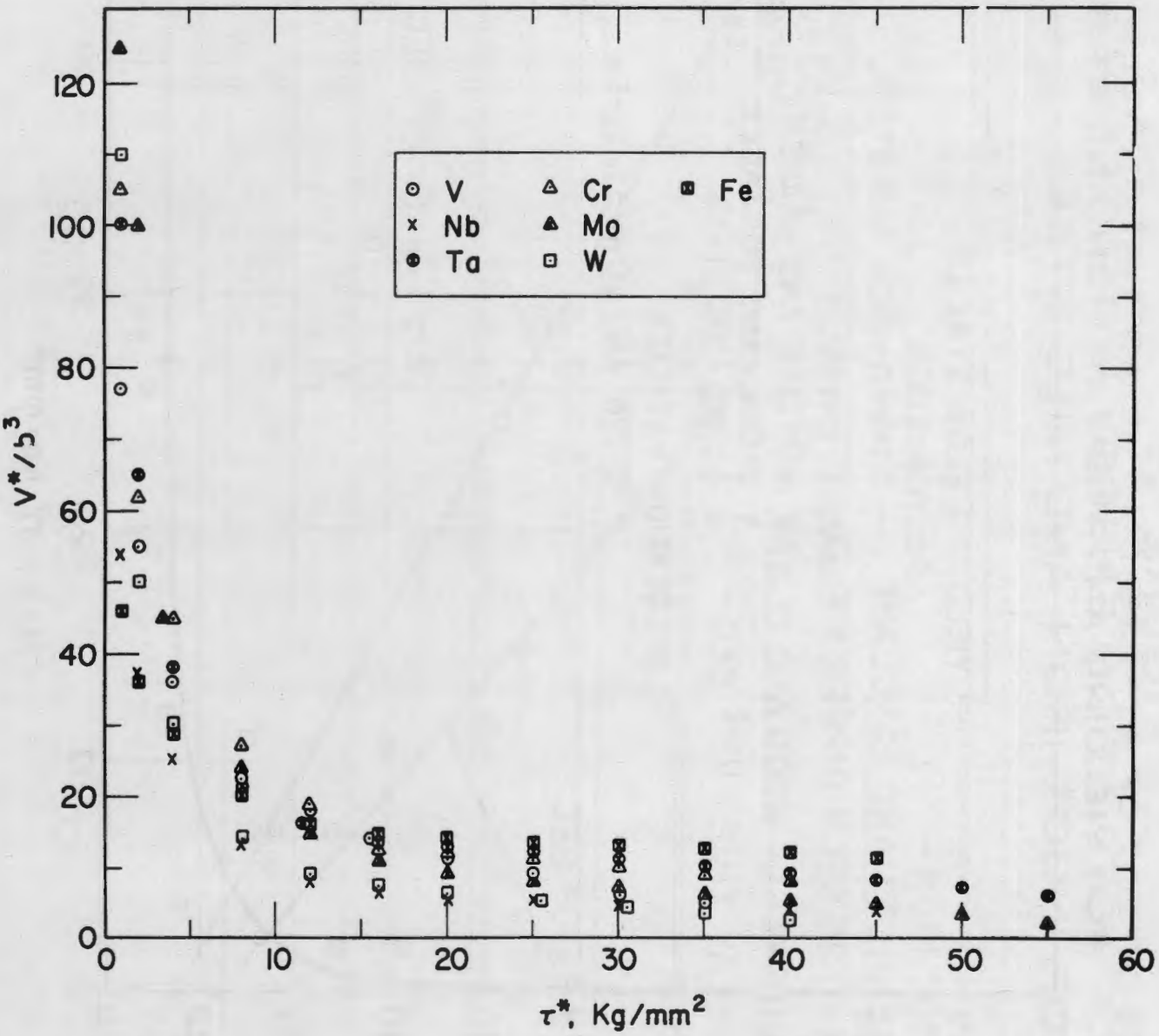

FIGURE 25

VARIATION OF ACTIVATION ENERGY WITH TEMPERATURE FOR INGOT IRON AND MILD STEEL

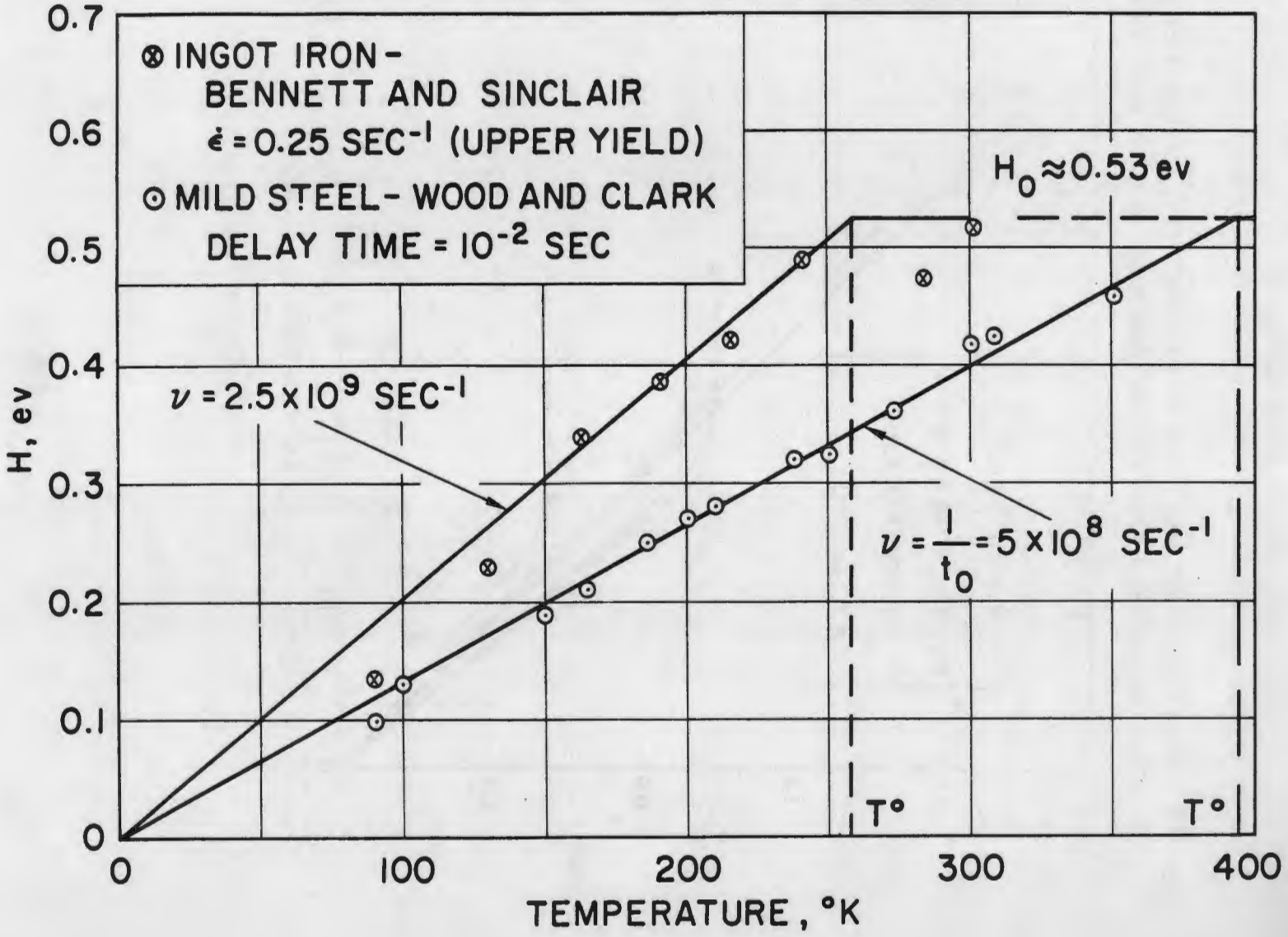

FIG. 26 VARIATION OF ACTIVATION ENERGY WITH TEMPERATURE FOR IMPURE, POLYCRYSTALLINE B.C.C. METALS

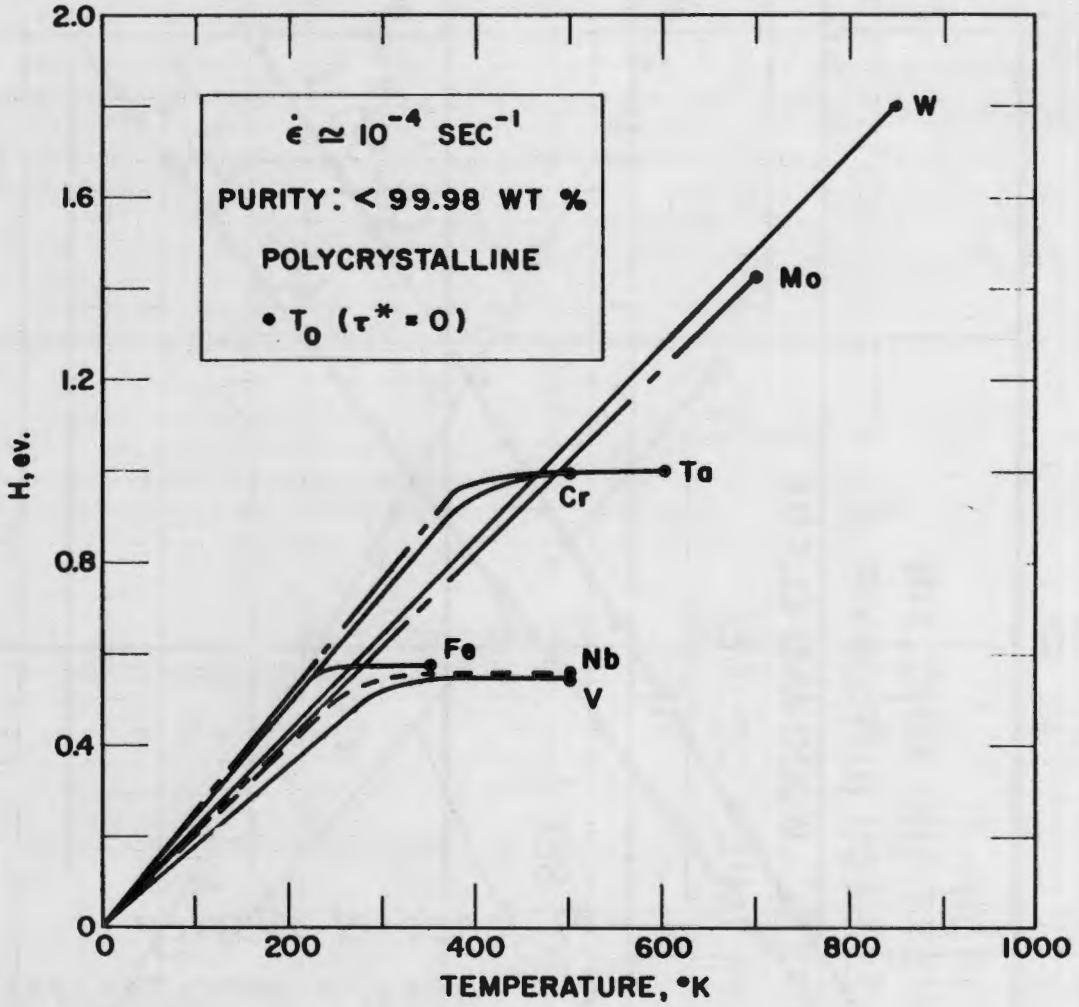

FIG. 27 VARIATION OF THE ACTIVATION ENERGY FOR BRITTLE FRACTURE WITH TEMPERATUE. (AFTER LEAN, PLATEAU AND CRUSSARD (38))

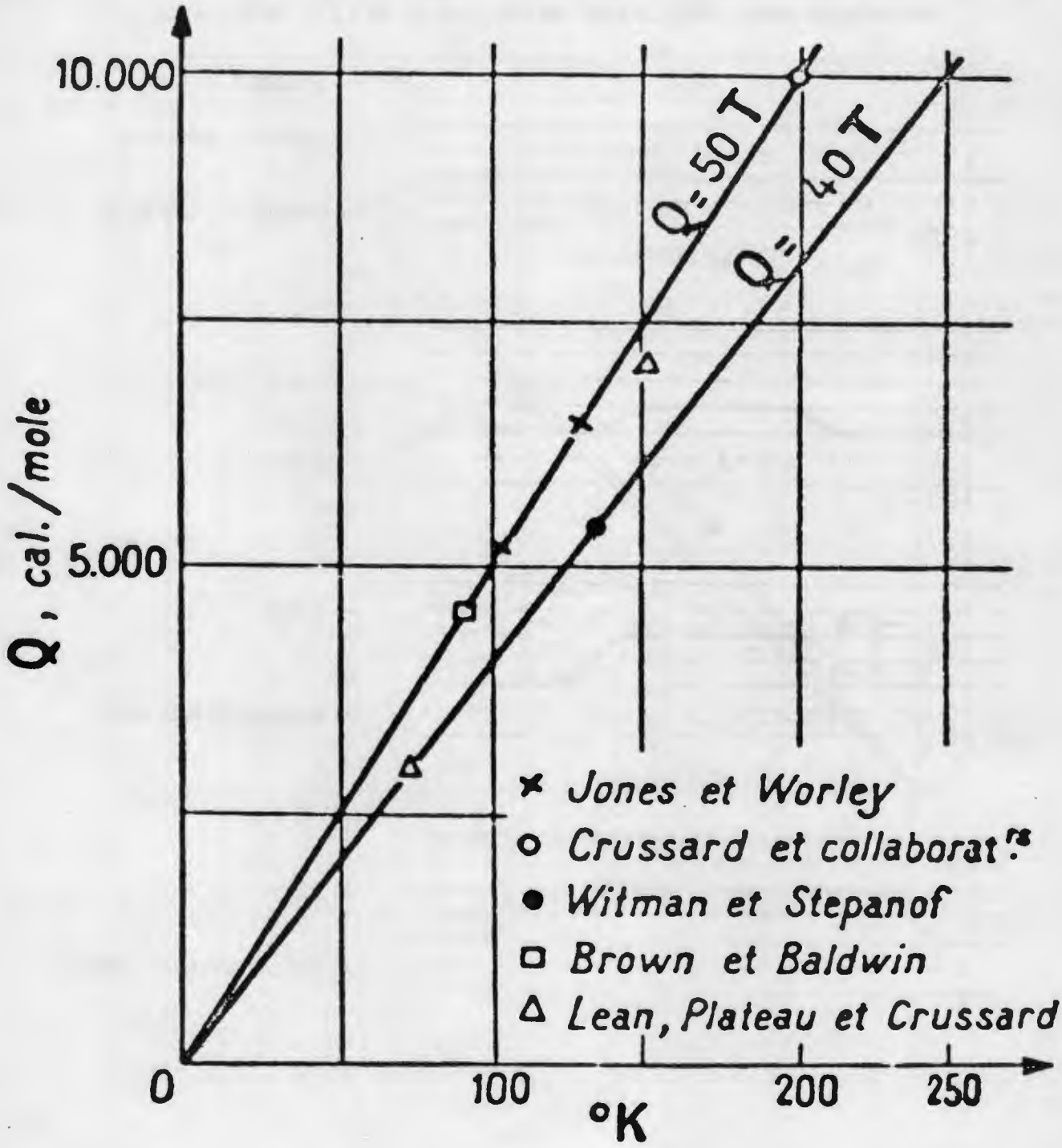

FIG. 28 SEEGER'S MODEL FOR THERMALLY-ACTIVATED OVERCOMING OF THE PEIERLS-NABARRO ENERGY. a. DISLOCATION LYING IN A CLOSE-PACKED DIRECTION. b. INTERMEDIATE STAGE IN THE FORMATION OF A PAIR OF KINKS OF OPPOSITE SIGN. c. FINAL STAGE IN THE FORMATION OF A PAIR OF KINKS. d. LATERAL MOTION OF THE KINKS UNDER THE APPLIED STRESS.

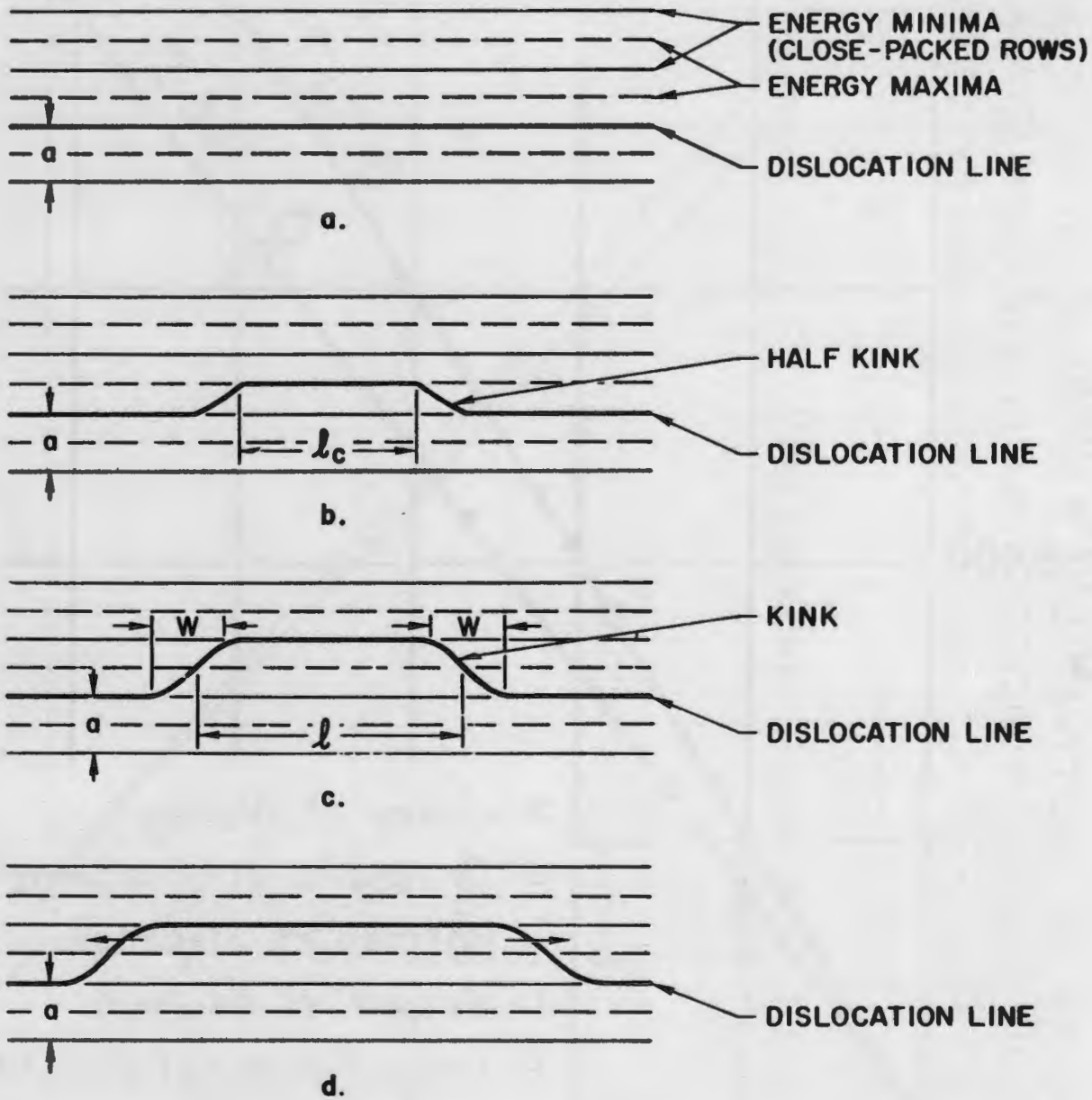

FIGURE 29

VARIATION OF ACTIVATION ENERGY WITH TEMPERATURE FOR ELECTROLYTIC IRON WATER QUENCHED FROM 920 C° (AFTER CONRAD AND FREDERICK (8))

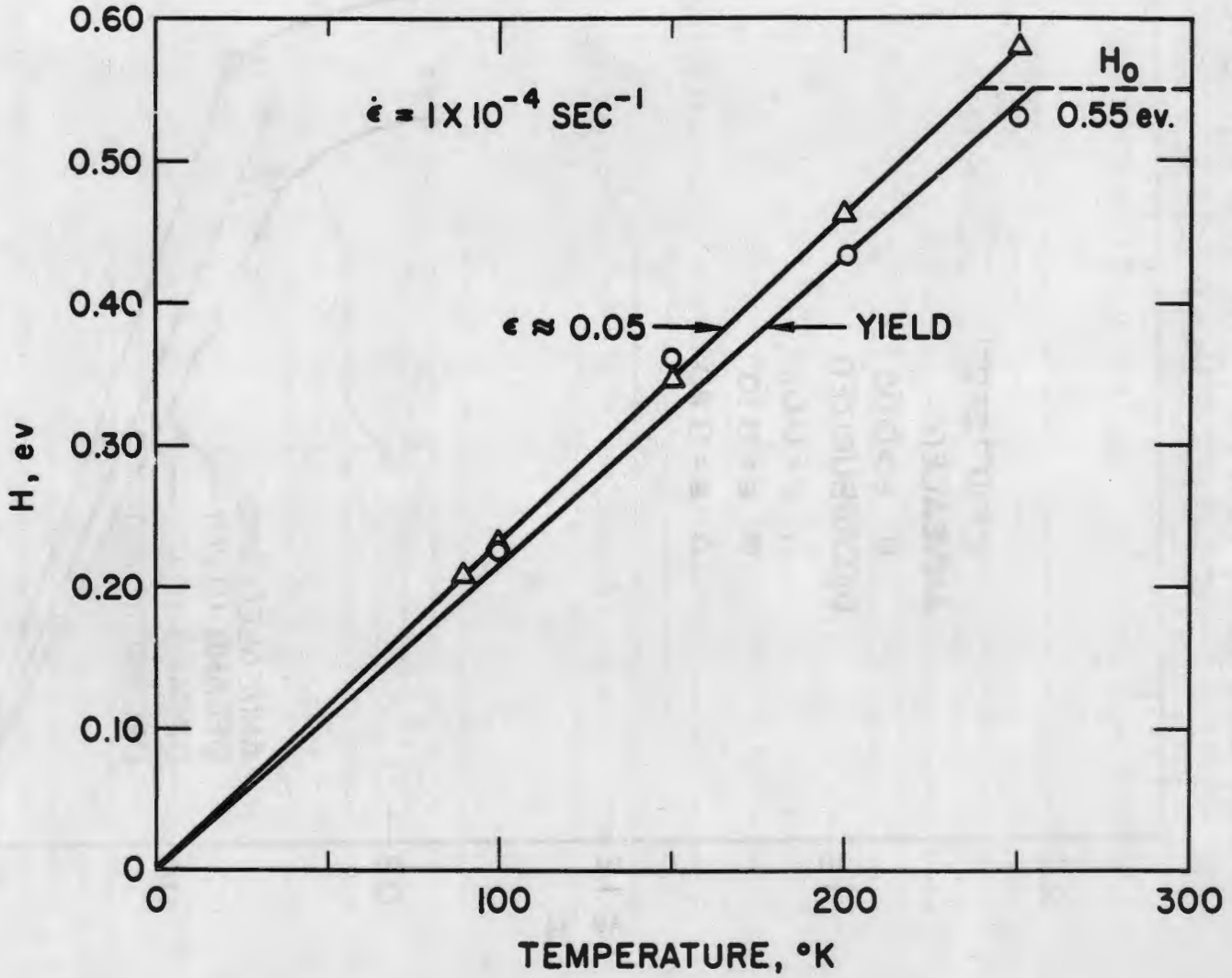

FIGURE 30

VARIATION OF ACTIVATION ENERGY WITH TEMPERATURE FOR FERROVAC IRON (FROM DATA OF BASINSKI AND CHRISTIAN (5)).

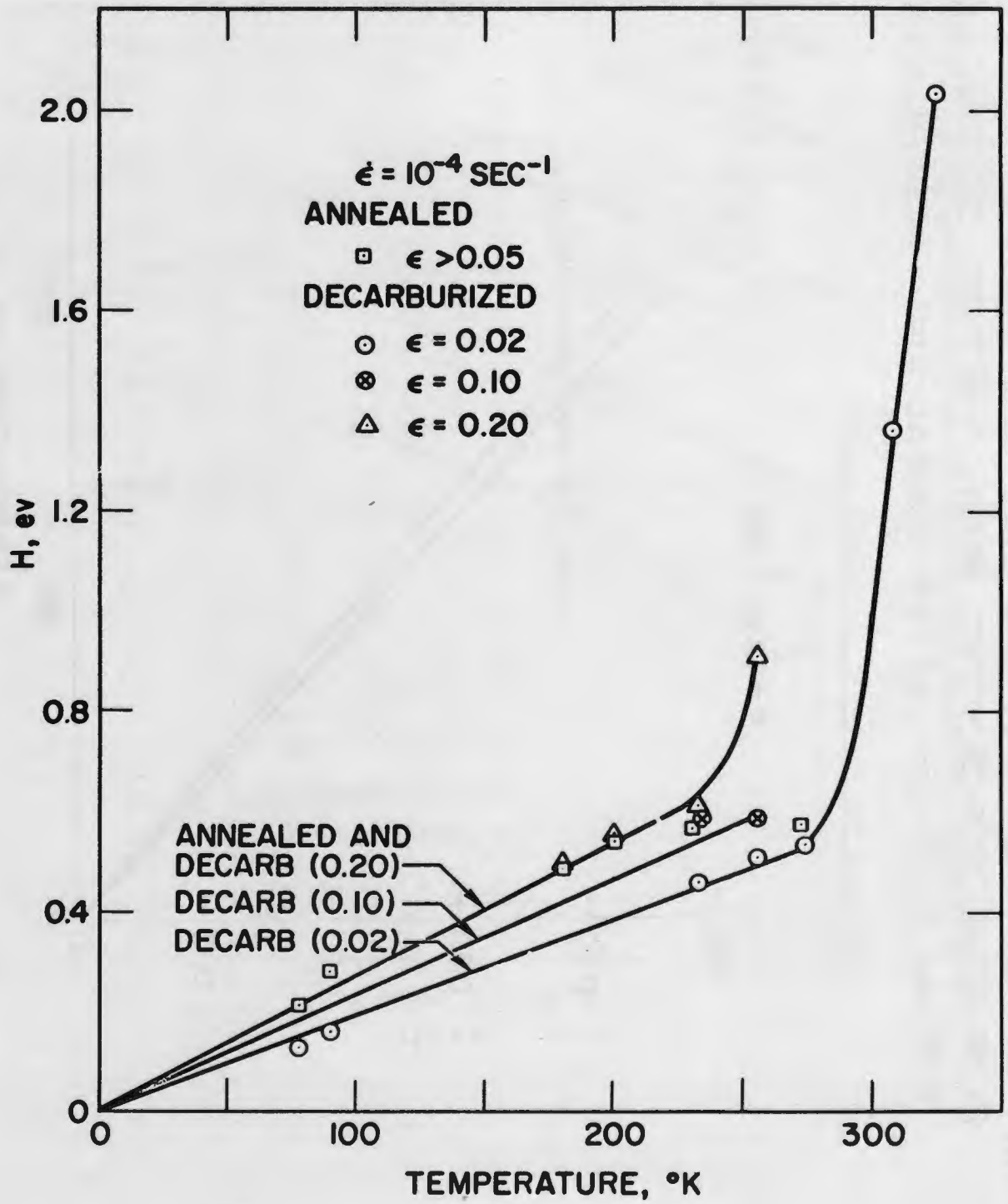

FIG. 31. COMPARISON OF CALCULATED AND EXPERIMENTAL STRESS-STRAIN CURVES FOR MILD STEEL